ADDIS ABABA UNIVERSTY

SCHOOL OF GRADUATE STUDIES

INSTITUTE OF TECHNOLOGY

SCHOOL OF MECHANICAL AND INDUSTRIAL ENGINEERING

FATIGUE FAILURE ON RAILWAY AXLE

A Thesis Submitted to the Graduate School of Addis Ababa University in partial fulfilment of

The requirements for the Degree of Masters of Science

In

Mechanical Engineering

(RAIL WAY STREAM)

By

Shoma Tadesse

Adivisors

Dr. Daniel Tilahun

Ato. Habtamu Tikubet

June 2017

ADDIS ABABA UNIVERSTY

SCHOOL OF GRADUATE STUDIES

INSTITUTE OF TECHNOLOGY

DEPARTMENT OF MECHANICAL ENGINEERING

Fatigue Failure on Railway Axle

Front Axle

By

Shoma Tadesse

June 2017

Approved by Board Examining

Daniel Tilahun (Dr.)	_____	_____
Chairman	Signature	Date
Daniel Tilahun (Dr.)	_____	_____
	Signature	Date
Ato: Habtamu Tikubet	_____	_____
Advisors	Signature	Date
	_____	_____
Internal Evaluator	Signature	Date
	_____	_____
External Evaluator	Signature	Date

ACKNOWLEDGEMENT

First of all I would like to thank my advisors Dr.Daniel Tilahun and Habtamu Tikubet for their grateful support and continuous advice of the work from the beginning up to the final result of the paper. I want to appreciate also their willingness and giving of motivations to work on research areas focusing on the current situations of the country, Ethiopia, pointing its future development and related problems to lay down the possible respective solutions. I would like to thank also to all people who stand on my side during the work of the paper. Especially, friends and colleagues who support and guide me during the Analysis of axle fatigue failure. Thanks also to engineer Yonus who is the mechanical engineer at Ethiopian Railway Corporation and helped me by giving the necessary materials to the possible outcomes of the research. Next, special thanks to my wife Alemnesh Debisa , Rabira Shoma and my family for their patience, support and motivation standing always on my side for the successful accomplishment of this paper and for the success of my life at all. Finally I thanks Zewditu Bersisa who help me by printing my thesis.

ABSTRACT

The purpose of the axle is one of the most important components of a rail vehicle which transmits the weight of the vehicle to the wheels, meets the vertical and horizontal loads formed during static and dynamic moving, and carries the driving moment and braking moment, since it is subjected to rotating bending and the issue of fatigue failure always exist .The main objective of this thesis is to one investigation of fatigue failure in railway front axle using finite element analysis. One of the most loaded axle locomotives are driving axles, which are subjected to simultaneous bending and twisting (while driving – especially during acceleration and braking) and the same bending (when stationary). Fatigue failures start at the most vulnerable point in a dynamically stressed area particularly where there is a stress raiser (discontinuities or change in diameter). Investigation and analyzing manually is tedious. Hence FEM is very accurate to analyzing and designing. FEM shows the most critical part of the axle to analyze the failures and also has available fatigue tool. Modeling of railway front axle to study fatigue failure under different loads using CATIA & ANSYS software is done. In addition parametric study to investigate the effect of loading condition in axles, estimation of fatigue life in working condition in railway front axle by finite element method using ANSYS Workbench software. By using FE M and numerical analysis the critical part of load that cause failure is investigated. Endurance limit, fatigue factor of safety and the theoretical no of cycles sustained by the axle before failure is estimated. In conclusion the increase in fillet radii of the axle and change in the position of the support decreases the stress concentration factor, increase the endurance limit and fatigue factor of safety of the axle.

Key word: Axle, Fatigue, ANSYS, stress concentration, railway vehicle axle bending

Contents

LIST OF TABLES

LIST OF FIGURES

SYMBOLS AND ACRONYMS

ACRONYMS

JIS Japan Industry Standards

SEM Scanning Electron Microscope

AAR The Association of American Railroads

HAZ Heat Affected Zone

VHCF Very High Cycle Fatigue

RPM Revolutions per Minute

EN European Norms

APDL ANSYS Parametric Design Language

AISI American Iron and Steel Institute

ASTM American Society for Testing and Materials

ASME American Society of Mechanical Engineers

SAE Automotive industry standards by many other industries

UIC = Union Internationale des Chemins de Fer (International Union of Railways)

SYMBOLS

M1 Mass on journals

g Acceleration due to gravity

P Half the vertical force per wheel set on the rail

P_1 Vertical force on the left of the journal

P_2 Vertical force on the right of the journal

Y_1 Wheel/rail horizontal force perpendicular to the rail on the left side

Y_2 Wheel/rail horizontal force perpendicular to the rail on the right side

H Force on the axle

Q_1 Vertical reaction on the wheel situated on the left side

Q_2 Vertical reaction on the wheel situated on the right side

F_i Forces of the unsprung elements situated between the two wheels (brake disc(s)

M_x Bending moment due to the masses in motion

M_x', Mz' bending moments due to braking

MX, MZ Sum of bending moments

MY Sum of torsional moments

MR Resultant moment

S distance between wheels treads to center of gravity

h_1 Height above the axle center line of vehicle center of gravity of masses carried

Yi Distance between the tread of one wheel and force Fi

μ Friction coefficient

σ Stress calculated in one section

K Fatigue stress concentration factor

R Nominal radius of the tread of a wheel

R_b Brake radius

LCF Low Cycle Fatigue

HCF High Cycle Fatigue

D diameter for one section of the axle

G Centre of gravity

FE function evaluation

I moment inertia of mass

J moment inertia of area

Chapter 1

INTRODUCTION

Railway axle is one of the most important components of railway vehicles, since it is subjected to rotating bending and the issue of fatigue failure always exists. The railway axles are usually designed for infinite life based on the endurance limit or fatigue limit of the material. An axle carries the vertical, lateral and horizontal loads formed during static and dynamic moving, and carries driving moment and braking moment. The weight of the railway vehicle is introduced to the axle via bearings mounted near the outer ends of the component. This leads to rotational bending of the axle while moving. Moreover, due to curving of the vehicle, asymmetric loading of the axles occurs, so that the axle part located closer to the outer curve radius is subjected to higher loading than the opposite axle part.

Fatigue in axle can generally be classified into three basic subdivisions: bending fatigue, torsional fatigue, and axial fatigue. Bending fatigue can result from these types of bending loads: unidirectional (one-way), reversed (two-way), and rotating. In unidirectional bending, the stress at any point fluctuates. Fluctuating stress refers to a change in magnitude without changing algebraic sign. In reversed bending and rotating bending, the stress at any point alternates. Alternating stress refers to cycling between two stresses of opposite algebraic sign, that is, tension (+) to compression (-) or compression to tension. Torsional fatigue can result from application of a fluctuating or an alternating twisting moment (torque). Axial fatigue can result from application of alternating (tension-and-compression) loading or fluctuating (tension-tension) loading.

Unidirectional-Bending Fatigue. The axial location of the origin of a fatigue crack in an axles subjected to a fluctuating unidirectional-bending moment evenly distributed along the length will be determined by some minor stress raiser, such as a surface discontinuity.

Reversed-Bending Fatigue: When the applied bending moment is reversing (alternating), all points in the axle are subjected alternately to tension stress and compression stress; while the points on one side of the plane of bending are in tension, the points on the opposite side are in compression. If the bending moment is of the same magnitude in either direction, two cracks of approximately equal length usually develop from origins diametrically opposite each other and often in the same transverse plane. If the bending moment is greater in one

direction than in the other, the two cracks will differ in length. Fatigue marks on the fracture surface of a stationary (nonrotating) axle subjected to a reversing bending moment evenly distributed along its length.

Rotating-Bending Fatigue: The essential difference between a stationary axle and a rotating axle subjected to the same bending moment is that in a stationary axle the tensile stress is confined to a portion of the periphery only. In a rotating axle, every point on the periphery sustains a tensile stress, then a compressive stress, once every revolution. The relative magnitude of the stresses at different locations is determined by conditions of balance or imbalance imposed on the axle. Another important difference introduced by rotation is asymmetrical development of the crack front from a single origin. There is a marked tendency of the crack front to extend preferentially in a direction opposite to that of rotation. A third difference arising from rotation is in the distribution of the initiation sites of a multiple-origin crack. In a nonrotating shaft subjected to unidirectional bending, the origins are located in the region of the maximum-tension zone. In a nonrotating shaft subjected to reverse bending, the origins are diametrically opposite each other. In rotary bending, however, every point on the axle periphery is subjected to a tensile stress at each revolution; therefore, a crack may be initiated at any point on the periphery.

Torsional Fatigue: Fatigue cracks arising from torsional stresses also show beach marks and ridges. Longitudinal stress raisers are comparatively harmless under bending stresses, but are as important as circumferential stress raisers under torsional loading. This sensitivity of axles loaded in torsion to longitudinal stress raisers is of considerable practical importance because inclusions in the axle material are almost always parallel to the axis of rotation. When a stress raiser such as a circumferential groove is present, different states of stresses exist around the stress raiser, and the tensile stress is increased to as much as four times the shear stress. The basic failure mechanism was fracture by torsional fatigue, which started at numerous surface shear cracks, both longitudinal and transverse that developed in the periphery of the root of the shear groove.

Mechanical stress raisers are non-uniformities in the shape of the axle such as step changes in diameter, sharp corners, keyways, grooves, threads, press-fitted or shrink-fitted members and surface discontinuities like seams, nicks, notches and machining marks. Crack initiation may also occur at other locations such as the transition region between the two principal diameters. Press-fitted elements such as wheel, disc or gear cause fatigue failure.

Steel is one of the most important materials in engineering and structural applications because of its high toughness, high strength and other outstanding mechanical properties compared with other materials. The material that will be observed in this paper is AISI 1050 steel.

1.1 Background

"Fatigue" was the name given to **mysterious** failure of locomotive axles over a century ago. Axles that were apparently sound would suddenly and catastrophically fail after several years of satisfactory service. Preliminary understanding about fatigue failure developed in 19th century during industrial revolution in Europe when heavy duty locomotives failed under cyclic loads.In,1839, Jean-Victor Poncelet, designer of cast iron axles for wheels, officially used the term fatigue for the first time in a book on mechanics. When railway systems began to develop rapidly in the middle of the nineteenth century, fatigue failures of railway axles became a widespread problem that began to draw attention to cyclic loading effects.

In1886, Johann Bauschinger wrote the first paper on cyclic stress- strain behavior of materials. By the end of 19th century, Gerber and Goodman investigated the influence of mean stress on fatigue parameters and proposed simplified theories for fatigue life. The phenomenon of fatigue was widely observed in 17th century during the failure of railway structures that claimed many lives, as reported by Gray and Smith .Thum and coworkers did initial research on the role of stress concentration on fatigue by investigating fatigue behaviour of shafts having rapidly varying cross-sections.

Today's design engineers in most industries are able to use different software based tools to predict durability with regard to the fatigue life of individual components. The tools from these software providers can help eliminate unexpected problems during product development which is critical, given the growing need for reduced costs and development time accompanied by an increase in quality requirements.

At the beginning of the 20th century, Sir James Alfred Ewing demonstrated the origin of fatigue failure in microscopic cracks and refuted the re-crystallization theory. This theory arose after one of the worst rail disasters of the 19th century occurred near Versailles in 1842, in which the leading locomotive broke an axle.

Figure 1-1 Broken Axles due to cyclic loading [5]

In the 1980's and 1990', more focus was put on investigating multi axial fatigue already being calculated with the help of computer technology. Increased digital prototyping with less testing has become a goal for the 21st century fatigue design. Today there are a wide variety of possibilities for predicting durability. ANSYS provides advanced fatigue analysis integrated within the ANSYS Workbench environment. Results and materials data from simulations within Workbench can be directly accessed by Design Life.

1.2 Motivation

Fatigue failure is a serious problem in Railway transport because it damage property and life.

- A desire to investigate fatigue failure to get save transport in railway
- Desire to solve fatigue problems and its approach
- Desire to understand causal relationships between load and its effects
- Provides an over view the beginning and growing of surface and subsurface initiated fatigue failure on railway front axle.

1.3 Research Problem

The fatigue failure is crucial in many areas of tribology. Railway axle is a component of Tribology so the fatigue failure of front axle has great influence on the efficiency of railways. Axle is an important element of railway to transmit a power in railway. The problem pertains to their failure at the journal bearings and between wheel and gear seat or on the body. Also the failure occurs at notch. Because of the static loads, especially during driving, braking and gear force it is necessary to perform appropriate fatigue calculations and to design the axle in such a way to obtain the required durability. In order to determine the cause of failure of the analyzed axle, the data have conducted in detailed to load analysis.

1.4 Objectives

General Objective

To investigate and analyses loads that contribute fatigue failure on railway front axle.

Specific Objectives

- 3D Modeling of axle to study fatigue condition by using CATIA & import to ANSYS software for analysis.
- To perform parametric study to investigate the effect of cyclic loading condition and material types in axle.
- To estimate fatigue failure in cyclic loading condition in axle by finite element method using ANSYS Workbench software.

1.5 Scope and Limitation

Fatigue life and the fatigue process are introduced. The fatigue life calculation is discussed briefly. Fundamental of fatigue design considerations, approach of fatigue design process and endurance limit modification to reduce the effect of mean stress is done. Safety factor is determined for whether the design is safe or not. Concept and cause of fatigue failure of railway axle is explained. Static structural analysis is covered in this thesis.

Limitation

Among the many, major obstacles while conducting this work were the followings;

- ❖ Materials such as no journals &literatures on front axles done.
- ❖ Experimental setups unavailability
- ❖ Lack of Research and literatures done on front axles.
- ❖ Lack of exact axle material in market and geometry

1.6 Research methodology

The research methodology for this study involved the following major tasks: literature review; discussion and comparison of different country standardization practice; and different data collection that contribute for standardization of guidelines for railway axle in Ethiopia.

Literature Survey: Literature survey of relevant material on railway axle has been done. The literatures available are from electronic media, journals, handbooks and books. The precise

dimensions have been used to translate in 2D and 3D drawing by using CATIA. Load analysis has been done. Load analysis calculated based on full load of passenger in the normal passenger vehicle. Later, value of load analysis has been applied on finite element analysis. 3D model of axle has been transfer to finite element Software which is ANSYS. Assigning material properties, load and meshing of the model has been done in this stages. Then, completed meshing model has been submitted for analysis. Finally an expected result from the static structural analysis has been obtained.

1.7 Organization

This work is organized in six chapters. The first chapter is devoted to brief description of fatigue failure of railway front axle; the thesis Introduction; background; problem of the statement; general and specific objectives. The second chapter presents literature review of fatigue failure of railway front axle. The third chapter Fatigue failure over view. The fourth chapter deals with axle design for fatigue of Railway Front axle. The fifth chapter addresses Results & Discussion. The last chapter devoted to draw conclusions, recommendations and future works.

Chapter 2

LITERATURE REVIEW

Historically fatigue failure of axles have been analyzed successfully with the use of beam manually, but even with the advent of computational tools such as finite element analysis, manual has not been analysis accurately the axles. More complex axles, hollow driving axles use finite element analysis. There are great deal of journals and number of literatures on fatigue failure of axles published. Generally their major concerns are on the analysis of fatigue stress, fatigue failure, crack growth in railway rear axles but yet no much literature review done on railway axle.

August Wöhler during 1860-1870 when he investigated failure mechanism of locomotive axles by applying controlled load cycles. He introduced the concept of rotating-bending fatigue test that subsequently led to the development of stress-rpm (S-N) diagram for estimating fatigue life and endurance or fatigue limit of metal, the fatigue limit representing the stress level below which the component would have infinite or very high fatigue life. Wöhler was also the first to arrive at the modern terms of “fatigue life” and “scatter” in the context of design for fatigue life. Besides developing the S-N curve, Wöhler also fabricated apparatus for repeated loading of axles. Based on the data obtained by Wöhler, Basquin represented the finite life region of the fatigue curve in the form of stress vs. number of load cycles on a double-log scale.

A study conducted by Hirakawa [5] in 1998 to study the effect of the diameter ratio between the press fitted parts and the journals on the fatigue strength of the press fitted parts of the railway axles. The results showed that in axles with small diameter ratios between the press-fitted parts and the plain sections, the press fitted parts are the fatigue critical parts. As the diameter ratio increases, the fatigue failure happens in the mid-span section of the axles. In Japanese axles, the diameter ratio (D/d), where D is the diameter of the wheel seat and d is the diameter of the plain part, is 1.10 and the critical parts are the press-fitted parts whereas in European axles, the diameter ratio (D/d) is 1.12 which makes the journals the fatigue critical parts. It is difficult to make the D/d sufficiently large if they are subjected to induction hardening.

Beretta and Carboni [2011] [6]: dealing with investigating the fatigue failure of railway axles can be referred which most of the failures start from the positions of stress concentrations

such as notches, defects, cracks and scratches. After manufacturing, various types of stress concentrators such as metallic and non-metallic inclusions, voids, defects and scratches are sometimes recognized in the axle that some of these discontinuities may lead to premature failure. Hence, derailment and other possible events may occur.

Alfredsson [8] develops a mechanism for surface initiated fatigue is based on tensile stresses. It is also realized that sub-surface initiated fatigue is the result of tensile residual stresses that emanate from plastic deformation below the surface. These mechanisms clearly show that contact fatigue cracks follow the same rules as ordinary fatigue cracks in hardened steel.

M. CARBONI [etal] [11] Summarize the crack initiation and growth in full scale railway axle in A1T mild steel have been studied, under three points rotating bending loading conditions and artificial rainwater as corrosive environment. A surface plastic replication technique has been used along with optical microscopy and scanning electron microscopy to monitor the environment assisted fatigue at various stages. The corrosion fatigue crack growth model enables us, also to obtain a fairly precise prediction of the S-N diagram of A1T steel under corrosion – fatigue sustained by the free corrosion of the material. The results indicated that at stress levels higher than the fatigue limit of the testing material in air, there was no significant difference between the fatigue strength of the samples tested in air and under artificial rainwater. But at stress levels below the endurance limit of the EA1N alloy in air, where cracks would not nucleate and propagate, the presence of a corrosive environment can assist the initiation and propagation of the cracks and lead to the premature fatigue failure of the samples.

M. MADIA [13] aim is a collection of stress intensity factor solution for cracks in railways axle geometries. These solutions comprise closed form analytical as well as tabled geometry functions they refer to solid as well as hollow axles and various crack sites such as the T-and V-notch and the axle body.

Rankine [14] investigated the fatigue failure of railway axles and suggested that the axles should be forged with a hub of enlarged diameter and large radii, so as to reduce the cutting of grain flows during machining, which would improve the fatigue life of axles. The axles are usually forged at high temperature before machining, therefore, it is difficult to attain precise dimensions and shape, so a large machining allowance is required resulting in a rough surface consisted of extensive irregular scratches.

Chapter 3

FATIGUE LOADING AND FATIGUE FAILURE IN AXLE

3.1 Fatigue Loading

Components are subjected to a variety of load (stress). Any loads that vary with time can potentially cause fatigue failure. The character of these loads may vary substantially from one application to another. The applied stress may be axial (tension-compression), flexural (bending), or torsional (twisting) in nature. In general, three different fluctuating stress–time modes are possible. One is represented schematically by a regular and sinusoidal time dependence. Reversed stress cycle, in which the stress alternates from a maximum tensile stress (+) to a maximum compressive stress (-) of equal magnitude. Where in the amplitude is symmetrical about a mean zero stress level, for example, alternating from a maximum tensile stress (σ_{max}) to a minimum compressive stress (σmin) of equal magnitude; this is referred to as a reversed stress cycle. In this study, the axle will be assumed experiencing the fully reversed for convenience. Thus, constant-amplitude load history can be represented by a constant load (stress) range, $\Delta\sigma$; a mean stress, σ_{mean}; an alternating stress or stress amplitude: $\pm_a(S_a)$; and a stress ratio, R. The stress range is the algebraic difference between the maximum stress, $\boldsymbol{\sigma}_{max}$ and the minimum stress, σ_{min} in the cycle.

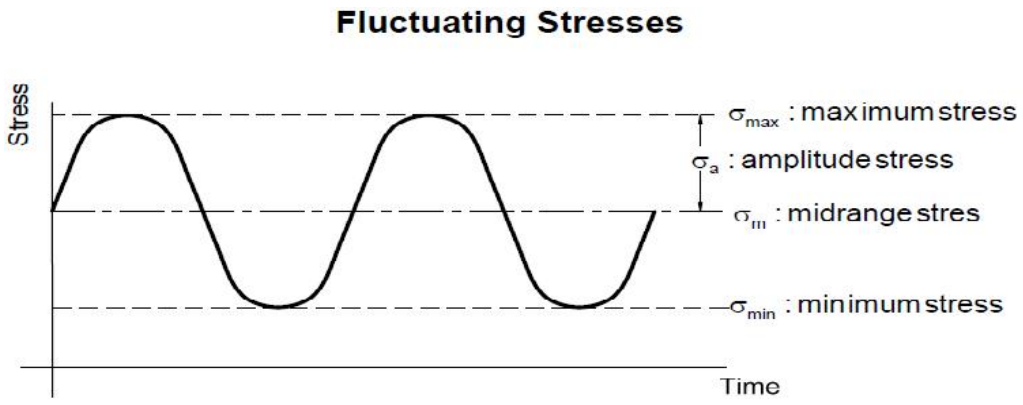

Figure 3-1 cyclic stress [7]

$$\Delta\pm = \pm_{Max} - \pm_{Min}. \quad \text{.....3.1}$$

The mean stress is the algebraic mean of σ_{max} and σ_{min} in the cycle

$$\pm_{mean} = \frac{(\pm_{max} + \pm_{min})}{2} \quad \text{.....3.2}$$

The alternating stress or stress amplitude is half the stress range in a cycle

$$\pm_{a} = S_{a} = \frac{(\Delta\pm)}{2} = \frac{(\pm_{max} - \pm_{min})}{2} \quad \text{.....3.3}$$

The stress ratio, R represents the relative magnitude of the minimum and maximum stresses in each cycle.

$$R = \frac{\pm_{min}}{\pm_{max}} \quad \text{----------3.4}$$

When the stress is fully reversed, then R = –1 and σmean = 0. These load patterns may result from bending, torsional, axial or a combination of these types of stresses.

3.2. Fatigue Classification

3.2.1 Subsurface initiated fatigue

The deterioration of the material is caused by cyclic loading and the built-up of stresses just underneath the raceway surface, ultimately resulting in decay of the material. Cracks are initiated and propagate underneath the surface, and when they come to the surface, spalling occurs. Bearings of axles under high Contact pressure, developing concentrated subsurface contact stresses that can cause surface pitting or Spalling after many cycles of the load. Pitting is a surface fatigue failure due to many repetitions of high contact stresses

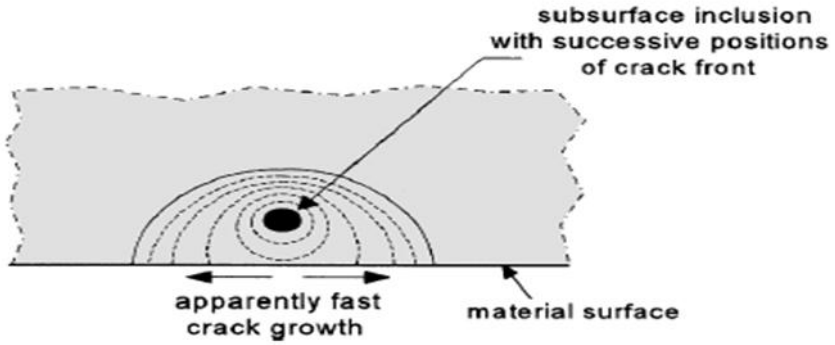

Figure 3-2 Subsurface nucleation growth [20].

The nucleation of a micro crack at an inclusion can occur slightly subsurface and not necessarily at the material surface. However, the free surface argument (lower restraint on slip) remains valid. It is for this reason that crack nucleation far below the material surface is rarely observed, although it can occur if the inclusion is large, or if a residual tensile stress

is present away from the material surface. An interesting situation arises if a micro crack initiated at a subsurface inclusion penetrates through the ligament between the inclusion and the free surface.

There are several mechanisms of sub-surface initiated cracks. Voskamp presents a mechanism based on tensile stresses that acts perpendicular to the contact surface of a ball in a raceway. Many materials contain stresses in them even though no external load is applied. Strictly, these stresses are not material properties, but they may influence apparent properties. Axles of heat-treated steel often contain tensile residual stresses just under the surface and compressive residual stress in the core. When such a bar is placed in a tensile tester, the applied tensile stresses add to the tensile residual stresses, causing fracture at a lower load than may be expected. Compressive residual stresses are formed in a surface that has been shot peened, rolled, or burnished to shallow depths or milled off with a dull cutter. Tensile residual stresses are formed in a surface that has been heated above the recrystallization temperature and then cooled (while the substrate remains unheated). Residual stresses imposed by any means will cause distortion of the entire part and have a significant effect on the fatigue life of solids. However, tensile stresses normal to the crack face are responsible for both surface and sub-surface initiated contact fatigue. The tensile stress appears during the unloading phase of an over-rolling sequence. Another mechanism that has been suggested for sub-surface fatigue is due to the shear stress amplitude. Phenomena like inclusions and porosity may also be crucial to initiation of sub-surface cracks.

3.2.2 Surface initiated fatigue

Vast majority of axle fatigue failures are caused by surface initiated fatigue cracks. This results from inadequate lubrication conditions. The role of the lubricant is to build up an oil film that separates the moving parts. Under poor lubrication conditions, for example due to contamination or inadequate viscosity, metal-to-metal contact occurs. The surface asperities (peaks) shear over each other, resulting in stresses that lead to material fatigue, and finally resulting in microspalls. Initially, there might be a shiny surface, because the surface roughness is reduced, but the process continues and the surface becomes dull and breaks up. Surface fatigue is the failure of a material as a result of repeated surface or sub-surface stresses beyond the endurance limit of the material.

3.3 Failure Mechanisms of Railway Axles

There are mainly two reasons for the failure of the railway axles:

- ❖Failure due to the overheating of the roller bearings
- ❖Failure due to the fatigue effect :

3.3.1 Failure due to overheating of the roller bearings

The overheating of roller bearings usually occurs as a result of the excessive friction caused by mechanical flaws or insufficient lubricant between the in contact surfaces. This situation is known as “The hot box” and the broken journal is referred to as “the burnt off journal”. The roller bearings of railway axles are composed of Babbitt material (any of the several alloys used for bearing surface) on Bronze backings. As a result of high temperatures, the Copper-based material of the bearings melt and cause the liquid metal embrittlement (LME) of the axles which lead to the formation of many short cracks on the axle surface. The overheated axles then break from the center of the overheated bearing assembly.

In this case, overheating of the bearings was caused as a result of sliding of the axles in them, which caused friction and warming up of the bearings. The brass cage of the bearings melted as a result of the temperature increase and flowed on the axle surface, which was heated up to austenitic region, leading to the formation of many small cracks on the surface of the axle as a result of liquid metal embrittlement. The cracks then propagated and led to the premature failure of the axle.

3.3.2 Failure due to the fatigue effect

Fatigue failure is believed to be the main failure mechanism for railway axles. Railway axles were among the first components which suffered from the fatigue damage and initiated the study on this surface effect. Fatigue is a structural damage that occurs when a material is subjected to cyclic loading. If the applied loads are above a certain threshold, microscopic cracks will begin to form from the surface. When a crack propagates and reaches a critical size, the fracture happens.

The fatigue behaviors of materials are described by their S-N curves also known as Wöhler curves. S-N curves show the magnitude of the cyclic stress (S) versus the logarithmic scale of number of cycles to failure at that stress (N). The S-N curves of some materials such as some steels and titanium alloys become horizontal at a particular stress limit which is called

"the fatigue limit" or "the endurance limit" of that material. The fatigue limit is a stress level under which there is no number of cycles that will cause failure. By keeping the applied loads on a component below its endurance limit an infinite life of that component can be maintained.

Railway axles are subjected to repeated loading cycles. The rotary bending stresses applied on axles cause an element of the material on the surface of the axles go from a compressive state to a tensile state which leads to fatigue of these components. The classical approach for the design of axles is based on the "safe life" methodology. The applied stresses on railway axles during service must be kept below the fatigue limit of axle material so that the fatigue cracks do not form. The axle dimensions and materials are chosen based on this methodology. It can be concluded that a simple way to keep the applied loads below the endurance limit of the axle material is to increase the diameter of the axles, but this is not practical since axles are considered as what is called "the unsprung mass" of the vehicle which must be minimized for better ride qualities and lower dynamic stresses.

One of the difficulties of the safe life design of axles is their fatigue limits. The fatigue limits of materials are defined at stress cycles in the range of 10^7, whereas the typical life of railway axles is about 30 years which is equal to about 10^9 cycles. At this number of cycles which corresponds to very high cycle fatigue (VHCF) the failure takes place at stress levels well below the defined fatigue limit of the material. The high number of cycles an axle experiences in service can lead to rotary bending fatigue failure.

Fatigue is a surface effect and starts from the surface. Any defects or stress concentrators on the surface of the axles can act as the crack initiation sites. It is known that the cracks on cylindrical components such as axle are in the form of semi-elliptical surface cracks. The crack initiation step is then followed by the crack propagation as the result of the loading of the axles. When a crack grows and reaches its critical size, the final fracture happens.

The crack initiation and propagation can occur by different mechanisms which are described in the following section. Other uncertainties about the applied loads on the axles, the effects of corrosion, flying ballast and wear are also some of the issues which make the safe life design of axles difficult. Fatigue is a surface effect and surface defects, subsurface inclusions, surface treatment and manufacturing process can alter the fatigue properties of components. Another cause that can lead to the premature fracture of the axles is the wearing of the axles which reduces the diameters which were chosen based on the required endurance limit for

the axles. That is why there are strict size limitations for railway axles and axles which are worn and under sized are replaced with new axles.

An axle consists of a plain part which is called “journal” and press fitted parts which include wheel seats, gear seats and brake seats. The critical parts of railway axles with regards to fatigue failure are either the press fitted parts which are the brake disk seats, gear seats and wheel seats, or the axle body close to notches and transitions.

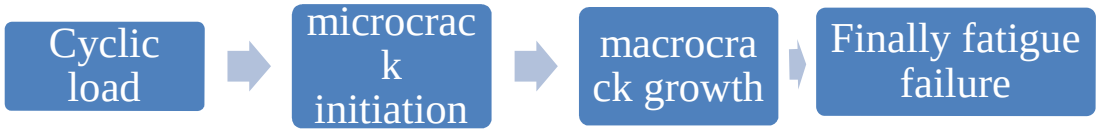

Figure 3-3 Process of fatigue failure

It implies that the crack growth period starts if the crack growth resistance of the material per *Se* is controlling the crack growth rate. The size of the micro crack at the transition from the initiation period to the crack growth period can be significantly different for different types of materials. The transition depends on microstructural barriers to be overcome by a growing micro crack, and these barriers are not the same in all materials. The crack initiation period includes the initial micro crack growth. Because the growth rate is still low, the initiation period may cover a significant part of the fatigue life.

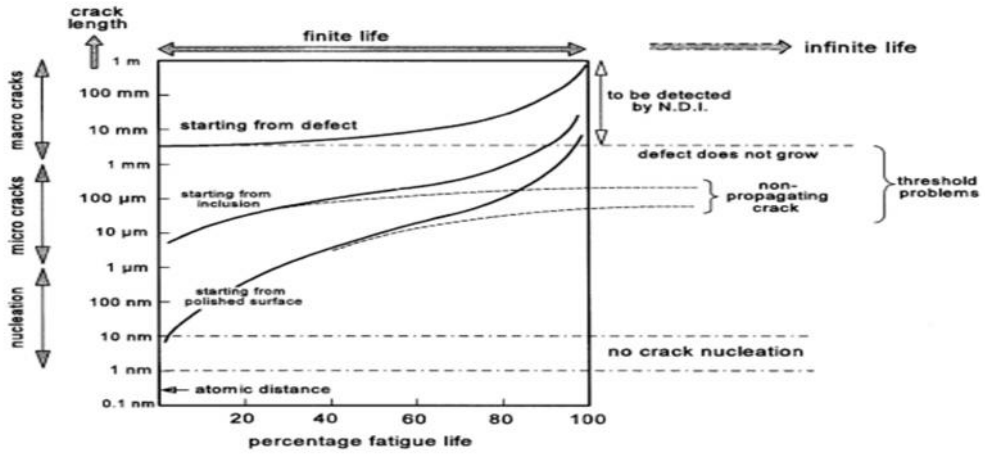

Figure 3-4 Different scenarios of fatigue crack growth. [19]

Which schematically shows the crack growth development as a function of the percentage of the fatigue life consumed (= n/N), with n as the number of fatigue cycles and N as the fatigue life until failure. Complete failure corresponds to n/N = 1 = 100%. There are three curves in Figure 3.1, all of them in agreement with crack initiation in the very beginning of the fatigue

life, however, with different values of the initial crack length. The lower curve corresponds to micro crack initiation at a “perfect” surface of the material. The middle curve represents crack initiation from an inclusion.

The upper curve is associated with a crack starting from a material defect which should not have been present, such as defects in a welded joint. The presence of defects can lead to sudden failure of the axles even far below the static strength limit. This is a major concern for axles that play an important role in a transportation industry such as railway [26]. Figure 3.41illustrates some interesting aspects:

(I) the vertical crack length scale is a logarithmic scale, ranging from

0.1 Nano meter (nm) to 1 meter (1 nanometer = 10^{-9} m). Micro cracks starting from a perfect free surface can have a sub-micron crack length (<1 «m = 10^{-6} m). However, cracks nucleated at an inclusion will start with a size similar to the size of the inclusion. The size can still be in the sub-millimeter range. Only cracks starting from macro defects can have a detectable macro crack length immediately.

(ii) The two lower crack growth curves illustrate that the major part of the fatigue life is spent with a crack size below 1 mm, i.e. with a practically invisible crack size.

(iii) Dotted lines in Figure 3.4 indicate the possibility that cracks do not always grow until failure.

3.4 Fatigue Failure Mode or Fatigue-Life Methods

- Stress-Life (S-N)
- Strain-Life (e-N)

Linear Elastic Fracture Mechanics Approach (LEFM)

Fatigue Regimes

- ✓ Low-cycle fatigue (LCF) less than 1000 cycles
- ✓ High-cycle fatigue (HCF) more than 1000 cycles

3.4.1 Stress-Life Approach

Stress Life is based on S-N curves (Stress – Cycle curves). Stress Life is concerned with total life and does not distinguish between initiation and propagation. In terms of cycles, Stress

Life typically deals with a relatively High number of cycles. High number of cycles is usually refers to more than 10^5 (100,000) cycles. Stress Life traditionally deals with relatively high numbers of cycles and therefore addresses High Cycle Fatigue (HCF), greater than 10^5 cycles inclusive of infinite life.

(a) Load amplitudes are predictable and consistent over the life of the part

(b) Stress-based model -determine the fatigue strength and/or endurance limit

(c) Keep the cyclic stress below the limit

3.4.2 Strain-Life Approach

Strain can be directly measured and has been shown to be an excellent quantity for characterizing low-cycle fatigue. Strain Life is typically concerned with crack initiation. Strain Life typically deals with a relatively low number of cycles and therefore addresses Low Cycle Fatigue (LCF), but works with high numbers of cycles as well. Low Cycle Fatigue usually refers to fewer than 10^5 (100,000) cycles. The Strain Life approach is widely used at present. For Strain Life, the total strain (elastic + plastic) is the required input. But, running an FE analysis to determine the total response can be very expensive and wasteful, especially if the nominal response of the structure is elastic so, an accepted approach is to assume a nominally elastic response and then make use of Neuber's equation to relate local stress/strain to nominal stress/strain at a stress concentration location.

(a) Gives a reasonably accurate picture of the crack-initiation stage

(b) Accounts for cumulative damage due to variations in the cyclic load

(c) Combinations of fatigue loading and high temperature are better handled by this methoda

(d) LCF, finite-life problems where stresses are high enough to cause local yielding

(e) Most complicated to use

3.4.3 Linear Elastic Fracture Mechanics Approach (LEFM)

Fracture Mechanics starts with an assumed flaw of known size and determines the crack's growth. Facture Mechanics is therefore sometimes referred to as "Crack Life"

Facture Mechanics is widely used to determine inspection intervals. For a given inspection technique, the smallest detectable flaw size is known.

Strain Life methods are used to determine crack initiation with Fracture Mechanics used to determine the crack life therefore: Crack Initiation + Crack Life = Total Life

3.5 Factors that affect fatigue life

- magnitude of stress (mean, amplitude or alternate stress)
- Mean stress – the average stress to which a component is subjected.
- Stress amplitude – the variation between the minimum and maximum stresses experienced in service.
- Quality of the surface (scratches, sharp transitions and edges).
- Thermal fatigue- thermal cycling causes expansion and contraction, hence thermal stress, if component is restrained.
- Corrosion fatigue-chemical reactions induce pits which act as stress raisers. Corrosion also enhances crack propagation.
- Frequency – how often the component is loaded and unloaded.
- Waveform – the variation in applied stress, perhaps a gentle rising and lowering or sudden shock changes.

3.5.1 Method to reduce those factors

- ✓ Polishing (removes machining flaws etc.)
- ✓ Introducing compressive stresses (compensate for applied tensile stresses) into thin surface layer by “Shot Peening”- firing small shot into surface to be treated. High-tech solution - ion implantation, laser peening.
- ✓ Case Hardening - create C- or N- rich outer layer in steels by atomic diffusion from the surface. Makes harder outer layer and also introduces compressive stresses
- ✓ Optimizing geometry - avoid internal corners, notches etc.
- ✓ Eliminate restraint by design
- ✓ Use materials with low thermal expansion coefficients
- ✓ Decrease corrosiveness of medium, if possible
- ✓ Add protective surface coating
- ✓ Add residual compressive stresses

Chapter 4

AXLE DESIGN FOR FATIGUE

The three main approaches in fatigue design philosophy, are Safe-Life, Fail-Safe and Damage-Tolerant.

A). Safe-Life (finite lifetime concept):- In the Safe-Life philosophy products are designed to survive a specific design life with a chosen reserve.

B). Fail-Safe (infinite lifetime concept):- Design to keep stress below threshold of fatigue limit, so as to reduce some of this waste of useful fatigue life, and maintain or improve the operating safety of a component in the later stages of its life.

C). Damage-Tolerant: - users need to inspect the part periodically for cracks and to replace the part once a crack exceeds a critical length. This approach usually uses the technologies of nondestructive testing and requires an accurate prediction of the rate of crack-growth between inspections. This is often referred to as damage tolerant design or "retirement-for-cause".

4.1 Material Selection

In the fields Rail vehicles, it is desired to further improve the mechanical strength of the axles and other power transmission components, in an attempt to satisfy increasing requirements for enhanced performance, increased horsepower and reduced weight. In this thesis work the material under study is AISI1050 steel, since it is commonly used in vehicle technology. AISI1050 steel is an alloy containing no other alloying element besides carbon. It is 0.5%C and carbon steel without alloying element besides carbon. It is medium alloy carbon steel. AISI1050 is an improved forging steel used for manufacture of axles which has improved strength and toughness while exhibiting enhanced machinability. This material suitably used for producing axle for vehicle for power transmissions. Many axles are made from low carbon, cold-drawn or hot-rolled steel, such as ANSI 1020-1060 steels should be considered first in most application. Have moderate to high strength with fairly good ductility. This material has Yield stress approaching those of the real axle will be selected from ANSYS material library to carry out the analysis of fatigue. In the end, material type will be set to AISI 1050. Due to the complete E-N curve data, and then E-N method is chosen to analyze fatigue failure of the locomotive axle. The fatigue analysis software ANSYS can

change stress-strain curve into strain. Meanwhile, it can correct the elastic stress-strain curve into cyclic stress-strain curve, and then elastic-plastic stress-strain curve is formed.

The reason behind that steel is selected for railway axle is as follows:

- Lightweight for easy handling.
- Superior Strength: All other materials talk about high strength, but their strength is still less than that of steel even when enhanced by steel reinforcing.
- Durability: One of the main reasons steel is used in so many construction projects is its durability—it has the highest strength-to-weight ratio of any other building material, making it ideal for buildings both large and small.
- Precise measurements, perfect angles.
- Great protection against the worst weather conditions.
- Steel Components mean minimal material waste.
- Labor costs are minimal.
- Steel is recyclable: Structural steel is the most recycled material on our planet – today's structural steel is made of 88% recycled product, is fully recyclable in the future and can be reused without further processing.
- Cost Effective.
- Material Cost are competitive
- Environmental Benefits: In addition to being one of the most durable materials available, steel products are also good for the environment. It is one of the few metals that is continuously recyclable, and any steel product that you use likely contains at least 25% recycled steel.

Table 4-1 chemical composition [www.litz-wire.com]

Material	%C	%Mn	%P	%S
AISI 1050	0.47-0.55	0.60-0.90	0.040	0.050

Table 4-2Physical properties of AISI 1050[www.litz-wire.com]

Physical properties	values
Ultimate strength(σ_{ut})	655Mpa
Yield strength(σ_y)	515Mpa
Young's modulus	205Gpa
Poisson's ratio(v)	0.290
density	7850kg/m^3

Materials for axles, method of axle strength, and types of Axles According to JIS

Table 4-3 Railway axle specification in JIS [36]

S/N	mark	Mechanical properties		Heat treatment
		YS(Mpa)	TS(Mpa)	
1	SFA55	>275	>540	Normalizing or normalizing &tempering
2	SFA60	>295	>590	Normalizing or normalizing &tempering
3	SFA65	>345	>640	Normalizing or normalizing &tempering
4	SFAQ	>275	>590	Induction heating QT

Locomotive axles are required to be annealed after forging and locomotive axles quenched and drawn. Axles are divided into four types. Types 1 to 3 are ones whose tensile strength has been increased by a suitable heat treatment, while Type 4 is an axle that has been subjected to induction heating and tempering after quenching and tempering. This means that the induction-hardened axles are much higher in fatigue strength than the European EA4T axles with proven performance. An induction-hardened axle having a large difference in diameter between the wheel seat and the axle body may be cited as a futuristic axle. If such an axle could be developed, it would become possible to significantly

reduce the diameter of the axle body (at present, this can hardly be done because of the limitations set by the induction hardening process), which in turn would make it possible to reduce the axle weight appreciably. In addition, as mentioned earlier, increasing the difference in diameter (i.e., diameter ratio) should help improve the fatigue strength of press-fitted parts. As for the chemical composition of steel materials for an axle, the JIS specifies only high limits of P and S as impurities. At present, medium-carbon steels (C: 0.30 to 0.48 mass%, Si: 0.15 to 0.40 mass%, Mn: 0.40 to 0.90 mass %) are used in Japan. In Europe, low-alloy steels added with Cr, Mo, etc., are also used.

4.1.1 Axle Geometry Layout

The general layout of an Axle to accommodate Axle elements, e.g. braking, bearings, and Wheels, must be specified in order to perform a free body force analysis and to obtain - moment diagrams. The geometry of an Axle is generally that of a stepped cylinder. The use of Axle shoulders is an excellent means of axially locating the Axle elements and to carry any thrust loads.

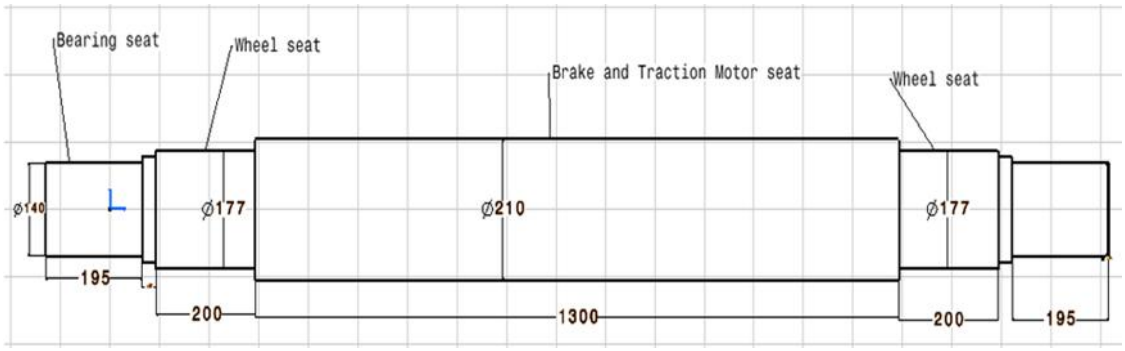

Figure 4-1 Geometric Layout of Axle

Table 4-4 Axle technical parameters [ERC]

gauge	*1435mm*
Axle load	*17 ton*
UIC standard axle	*200kg*
speed	*120km/h*
Vehicle center distance	*1040mm*
axle length(UIC)	*2180mm*

4.1.2 Failure Theory

Design of axle for fluctuating load (reversed bending with reversed torsion) calculated von-Mises stress. The Distortion energy theory for fatigue failure analysis to find maximum stress values because there is combined loading of bending and torsion. Distortion energy theory is used when the factor of safety is to be held in close limits and the cause of failure of the component is being investigated. This theory predicts failure most accurately for ductile material. But design calculations involved in this theory are slightly complicated as compared with other theories of failure.

Bending, torsion, and axial stresses may be present in both midrange and alternating components [Fatigue design handbook, 3rd ed. York: SAE; 1997]. For analysis, it is simple enough to combine the different types of stresses into alternating and midrange von-Mises stresses. The presence of a mean-stress component has a significant effect on failure. When a mean component of stress is added to the alternating component, (repeated) and (fluctuating) the material fails at lower alternating stresses than it does under fully reverse loading. Axial loads are usually comparatively very small at critical locations where bending and torsion dominate, so they will be left out of the following equations. In this section, calculated the von-Mises (equivalent) stress $(\pm\ _{eq})$, factor of safety (f_s), Number of cycles (N) respectively.

Initially, calculate Maximum and minimum bending moments at different points. The bending moment and twisting torque at each part of the axle are obtained from all the forces acting upon the axles during locomotive operation, including the weight and inertia force of the car body and bogies, the reaction force from the wheels, the forces from the driving and braking units, the forces applied via the bogie frame, etc.

Next, the bending moment and twisting torque obtained are converted into the bending stress and twisting stress, respectively, by using a technique based on the strength of materials theory. With respect to the allowable bending stress, it is prescribed for each type of axle material and each axle part. For the rotating bending fatigue limit of small test pieces, consideration is given to not only the size effect but also the fitting effect for each fitted part or the surface roughness effect for each non-fitted part. The twisting elastic limit is used as the allowable twisting stress because a twisting stress occurs less frequently than a bending stress, and there is a phase difference between the bending stress and twisting stress. The safety factor of each of the axle parts is calculated using the formula. This is to take the effect

of superposition of bending stress and twisting stress into account. For each of the axle parts, a reference safety factor has been decided with due consideration given to the difference in vehicle types. The fluctuating stresses due to bending and torsion are given by:-

$$M_m = \frac{(M_b)\max + (M_b)\min}{2} \quad \text{..... 4.1}$$

$$M_a = \frac{Mb_{max} - Mb_{min}}{2} \quad \text{.....4.2}$$

$$\sigma_a = \frac{k_f * M_a c}{I} \quad \text{..... (4.3)}$$

$$where, I = \frac{\pi d^4}{64}, c = \frac{d}{2}$$

$$\tau_a = \frac{k_{fs} * T_a c}{J} \quad \text{.....} \quad (4.4)$$

$$where \ , \ j = \frac{\pi r^4}{2} = \frac{\left(\frac{d}{2}\right)^4}{2} = \frac{\pi d^4}{32}$$

$$\sigma_m = \frac{k_f * M_m c}{I} \quad \text{..... (4.5)}$$

$$\tau_m = \frac{K_{fs} * T_m c}{J} \quad \text{..... (4.6)}$$

Where M_m and M_a are the midrange and alternating bending moments, T_m and T_a are the midrange and alternating torques, and K_f and K_{fs} are the fatigue stress concentration factors for bending and torsion, respectively. j=polar moment inertia of an area and I=moment inertia of mass.

$$\sigma_a = \frac{k_f * 32 M_a}{\pi d^3} \quad \text{..... (4.7)}$$

$$\sigma_m = \frac{k_f * 32 M_m}{\pi d^3} \quad \text{..... (4.8)}$$

$$\tau_a = \frac{k_{fs} * 16 T_a}{\pi d^3} \quad \text{..... (4.9)}$$

$$\tau_m = \frac{k_{fs} * 16 T_m}{\pi d^3} \quad \text{..... (4.10)}$$

Combining these stresses in accordance with the distortion energy failure theory, the von Mises stresses for rotating round, solid shafts, neglecting axial loads, are given by [shigle 8 edition page 354-402]:

$$\sigma'_a = (\sigma_a^2 + 3\tau_a^2)^{1/2} = [(32k_f m_a/\pi d^3)^2 + 3(16k_{fs} T_a/\pi d^3)^2]^{1/2} \quad (4.11)$$

$$\sigma'_m = (\sigma_m^2 + 3\tau_m^2)^{1/2} = [(32k_f m_m/\pi d^3)^2 + 3(16k_{fs} T_m/\pi d^3)^2]^{1/2} \quad (4.12)$$

Note that the stress concentration factors are sometimes considered optional for the midrange components with ductile materials, because of the capacity of the ductile material to yield locally at the discontinuity.

These equivalent alternating and midrange stresses can be evaluated using an appropriate failure curve on the modified Goodman diagram. For example, the fatigue failure criteria for the modified Goodman line as expressed is

$$\frac{1}{n_f} = \frac{\sigma'_a}{S_e} + \frac{\sigma'_m}{S_{ut}}$$

Substitution of $\sigma'_a$and σ'_m from Eqs. (9) and (10) results in

$$\frac{1}{n} = \frac{16}{\pi d^3}\{\frac{1}{S_e}[4(K_f M_a)^2 + 3(K_{fs} T_a)^2]^{1/2} + \frac{1}{S_{ut}}[4(K_f M_m)^2 + 3(K_{fs} T_m)^2]^{1/2}\} \quad (4.13)$$

For design purposes, it is also desirable to solve the equation for the diameter.

$$d = (\frac{16}{\pi}\{\frac{1}{S_e}[4(K_f M_a)^2 + 3(K_{fs} T_a)^2]^{1/2} + \frac{1}{S_{ut}}[4(K_f M_m)^2 + 3(K_f T_m)^2]^{1/2}\})^{1/3} \quad (4.14)$$

Similar expressions can be obtained for any of the common failure criteria by substituting the von Mises stresses from Eqs. (4.9) and (4.10) into any of the failure criteria expressed. The resulting equations for several of the commonly used failure curves are summarized below. The names given to each set of equations identifies the significant failure theory, followed by a fatigue failure locus name. For example, DE-Gerber indicates the stresses are combined using the distortion energy (DE) theory, and the Gerber criteria are used for the fatigue failure.

DE-Goodman

$$\frac{1}{n} = \frac{16}{\pi d^3}\{\frac{1}{S_e}[4(k_f M_a)^2 + 3(K_{fs} T_a)^2]^{1/2} + \frac{1}{S_{ut}}[4(K_f M_m)^2 + 3(K_{fs} T_m)^2]^{1/2}\} \quad (4.15)$$

$$d = (\frac{16n}{\pi}\{\frac{1}{S_e}[4(k_f M_a)^2 + 3(K_{fs} T_a)^2]^{1/2} + \frac{1}{S_{ut}}[4(K_f M_m)^2 + 3(K_{fs} T_m)^2]^{1/2}\})^{1/3} \quad (4.16)$$

DE-Gerber

$$\frac{1}{n} = \frac{8A}{\pi d^3 S_e}\{1 + [1 + (\frac{2BS_e}{AS_{ut}})^2]^{1/2}\} \quad (4.17)$$

$$d = (\frac{8nA}{\pi S_e}\{1 + [1 + (\frac{2BS_e}{AS_{ut}})^2]^{1/2}\})^{1/3} \quad (4.18)$$

Where:-

$$A = \{4(K_f M_m)^2 + 3(K_{fs} T_a)^2\}^{1/2}$$

$$B = \{4(K_f M_m)^2 + 3(K_{fs} T_a)^2\}^{1/2}$$

$$d = \frac{16n}{\pi}\{[4(\frac{f_f M_a}{S_e})^2 + 3(\frac{K_{fs} T_a}{S_e})^2 + 4(\frac{K_f M_m}{S_y})^2 + 3(\frac{K_{fs} T_m}{S_y})^2]^{1/2}\}^{1/3} \quad \text{(4.19)}$$

DE-Soderberg

$$\frac{1}{n} = \frac{16}{\pi d^3}\{\frac{1}{S_e}[4(k_f M_a)^2 + 3(K_{fs} T_a)^2]^{1/2} + \frac{1}{S_{yt}}[4(K_f M_m)^2 + 3(K_{fs} T_m)^2]^{1/2}\} \quad \text{(4.20)}$$

$$d = (\frac{16n}{\pi}\{\frac{1}{S_e}[4(k_f M_a)^2 + 3(K_{fs} T_a)^2]^{1/2} + \frac{1}{S_{yt}}[4(K_f M_m)^2 + 3(K_{fs} T_m)^2]^{1/2}\})^{1/3} \quad \text{(4.21)}$$

For a rotating shaft with constant bending and torsion, the bending stress is completely reversed and the torsion is steady. Equations (4.13) through (4.20) can be simplified by setting M_m and T_a equal to 0, which simply drops out some of the terms.

Note that in an analysis situation in which the diameter is known and the factor of safety is desired, as an alternative to using the specialized equations above, it is always still valid to calculate the alternating and mid-range stresses using Eqs. (4.11) and (4.12), and

Solve directly for "n".

A von Mises maximum stress is calculated for this purpose.

$$\sigma'_{max} = [(\sigma_m + \sigma_a)^2 + 3(\tau_m + \tau_a)^2]^{1/2} = [\frac{32k_f M_m + M_a}{\pi d^3}^2 + 3\frac{16k_{fs} T_m + T_a}{\pi d^3}^2]^{1/2} \quad \text{(4.23)}$$

To check for yielding, this von-Mises maximum stress is compared to the yield strength, as usual.

$$n_f = \frac{S_y}{\sigma'_{max}} \quad \text{(4.24)}$$

For a quick, conservative check, an estimate for σ′ max can be obtained by simply adding σ'_a and σ'_m ($\sigma'_a + \sigma'_m$) will always be greater than or equal to σ'_{max}, and will therefore be conservative.

4.2Analysis Using Analytic Method

4.2.1 Force analysis of Wheels and Axle

A vertical force is applied near each end of the axle via a bearing, while a reaction force (also in vertical direction) is applied to the surface of contact between the axle and rail.

No direct contact between axle and rail. The load is distributed through the following:

Side bearing → upper spring beam → secondary suspension →suspension link → hanger link → hanger block → primary spring →axle box wing→ journal→ bearing →axle →wheel →Rail . In addition, in a curved railway section, a lateral force produced by the contact between the wheel and rail is applied toward the outer rail. At this moment, the wheel set is put under the rotational bending stress. All the contributions to the bending moment, from masses, braking and traveling in curve, have to be considered; forces in the longitudinal direction and at contact can be neglected;

4.2.2 Types of forces

Types of forces are to be taken into consideration as a function:

1) Of the masses in motion;

2) Of the braking system.

3) Of gear force

4.2.3 Effects due to masses in motion

The higher contribution to resultant moment comes from forces due to masses in motion. The conventional vertical loads are expressed as function of m_1, the mass on journals per wheel set (bearing & axle boxes included). The value of m_1, refers to mass in service of the vehicle, computed with all vehicles and the mass of passengers depending on the kind of vehicle.

The analytic expression are derived imposing the static balance of the wheel set, under normal accelerations acting on the center of gravity of suspended masses of vehicle; the nominal acceleration are related to the typology of axle (powered or not powered) to operational conditions (axle guiding or not guiding) and typology of train (tilting or not). The result is that the coefficients, defining these conventional loads, change depending on typology of the axle .Considering as an example a train of a non-tilting vehicle, the

expression for forces P_1 and P_2 acting on journals derive from an estimation of lateral acceleration equal to 0.15g, computed simultaneously with an increment on both journals of 25% of half the static load m_1g acting on them. [EN13104]. P_o is a Vertical static force per journal when the wheel set is loaded symmetrically $\frac{M_1 g}{2} = 0.5 M_1 g$.

When increment is 25 %(0.25), $0.25 * 0.5 M_1 g = 0.125 M_1 g$

$$P_1 = 0.5M_1g + 0.125M_1g + 0.0875\left(\frac{h_1}{b}\right)M_1g = \left[0.625 + 0.0875\left(\frac{h_1}{b}\right)\right].M_1g \quad \text{.....4.25}$$

$$P_2 = 0.5M_1g + 0.125M_1g - 0.0875\left(\frac{h_1}{b}\right)M_1g = \left[0.625 - 0.0875\left(\frac{h_1}{b}\right)\right]M_1g \quad \text{.....4.26}$$

$$Y_1 = \frac{W}{2}\frac{V^2}{R} - \frac{C}{G} \quad \text{.....4.27}$$

$$Y_2 = -\frac{W}{2}\frac{V^2}{R} - \frac{C}{G} \quad \text{.....4.28}$$

Y_1=quasi static lateral force at outer rail [N]

Y_2=quasi static lateral force at inner rail [N]

V=running velocity of vehicle [km/h] =$19.44\ \frac{m}{s}$

W=axle load [KN] =$83400N$

R=curve radius [m] =145m

C=design super elevation or cant [m] =0.15m

G=track gauge [m] =1.435m

Once P_1 and P_2 is identified from static balance of equations for the masses suspended on journals , the other forces necessary for the calculation of the bending moment M_x can be derived from static balance equations of the wheel set. F_i is the forces exerted by the masses of the unsprung elements located between the two wheels, typically brake discs. The forces generated by masses in motion are concentrated along the vertical symmetry

plane (y, z) (see Figure4.2) intersecting the axle center line

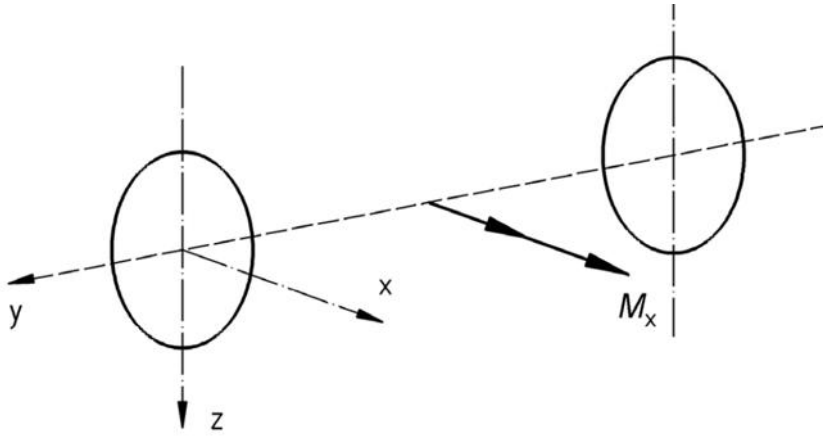

Figure 4-2Forces generated by masses in motion

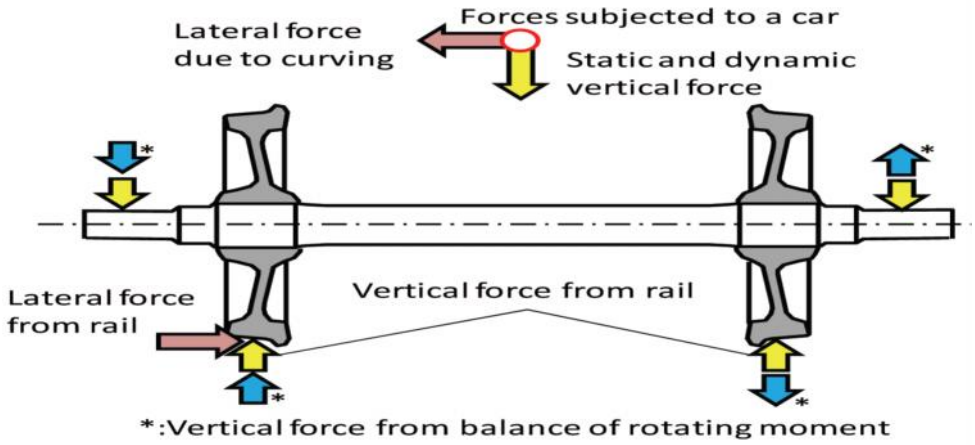

Figure 4-3 Forces subjected to a wheel-axle assembly [EN13104].

Figure above shows the external forces that act upon a wheel set. As shown, a vertical force is applied near each end of the axle via a bearing, while a reaction force (also in vertical direction) is applied to the surface of contact between the axle and rail. In addition, in a curved railway section, a lateral force produced by the contact between the wheel and rail is applied toward the outer rail. At this moment, the wheel set is put under the typical rotational bending stress.

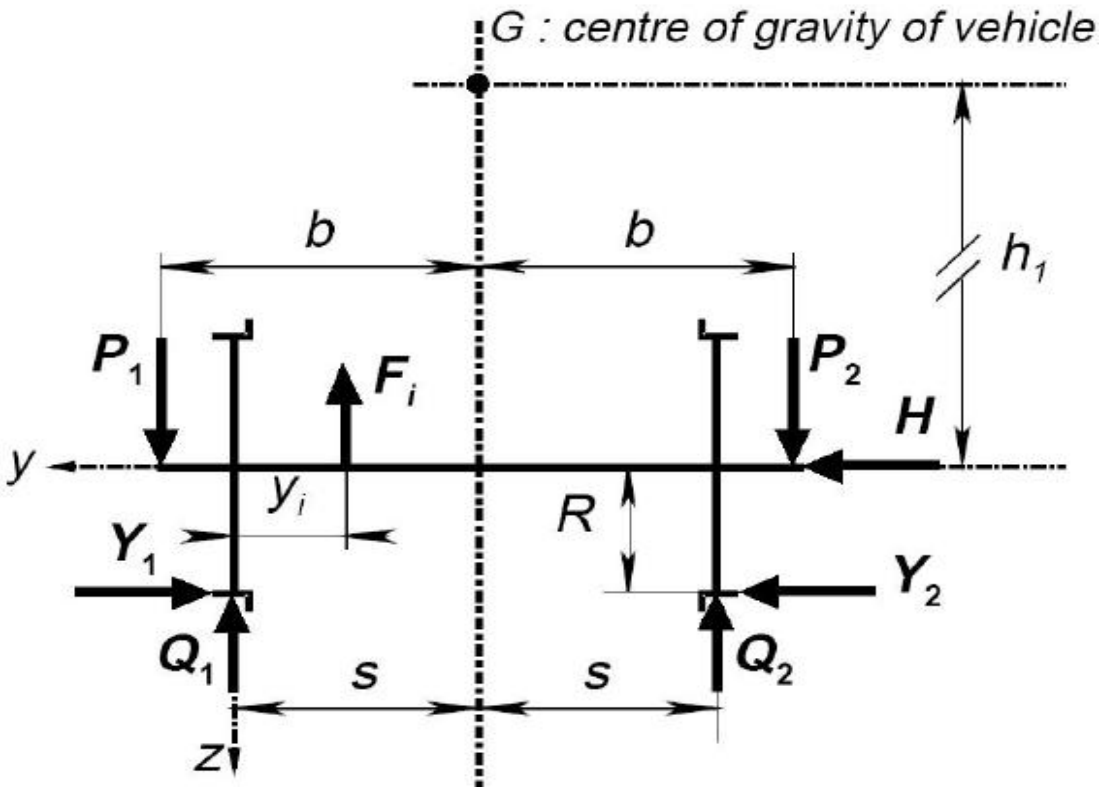

Figure 4-4 Force distribution on the Axle and Wheels

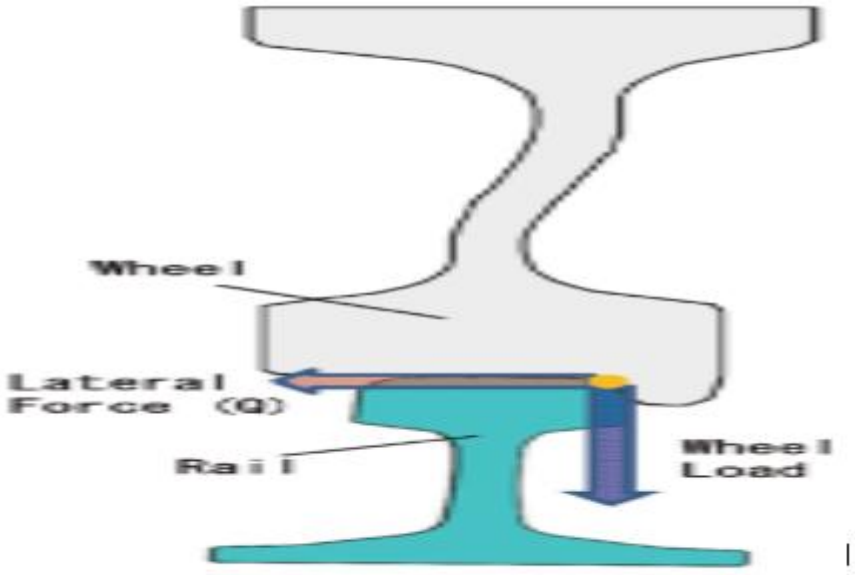

Table 4-5 Formulae's used for Theoretical Calculations [EN13104]

For all axles defined in the scope of this standard[EN13104]	$P_1 = (0.625 + 0.0875\ h_1 / b)\ m_1\ g$ $P_2 = (0.625 - 0.0875\ h_1 / b)\ m_1\ g$ $Y_1 = 0.35\ m_1\ g$ $Y_2 = 0.175\ m_1\ g$ $H = Y_1 - Y_2 = 0.175\ m_1\ g$ $Q_1 = \left[\frac{P_1(b+s) - P_2(b-s) + (Y_1 - Y_2)R_w - \sum_i F_i(2s - y_i)}{2s} \right]$ $Q2 = \left[\frac{P_2(b+s) - P_1(b-s) - (Y_1 - Y_2)R_w - \sum_i F_i y_i}{2s} \right]$

P_1 Vertical force on the left of the journal

P_2 Vertical force on the right of the journal

Y_1 Wheel/rail horizontal force perpendicular to the rail on the left side

Y_2 Wheel/rail horizontal force perpendicular to the rail on the right side

H Force on the axle

Q_1 Vertical reaction on the wheel situated on the left side

Q_2 Vertical reaction on the wheel situated on the right side

F_i Forces of the unsprung elements situated between the two wheels (brake disc(s)

From the ERC:-total mass=m_1 = 8500kg

Height= h_1 = 1040mm[from standard, EN 1990]

Length, b = 978mm and The standard track gauge is 1435 mm and for this gauge the distance between the points of contact of the mean wheel circles with the rails, tack width 2 S is 1500 mm (Esveld, 2001) and s = 750mm

Wheel radius R_w = 457.5mm[ERC]

Brake force= F = 41.6kN[UIC CODE – 541-3.]

V = $120\frac{\text{Km}}{\text{hr}}$ From ERC obtained.

Calculate angular speed "w"

$$V = wR_{wheel} \rightarrow w = \frac{V}{R_{wheel}} = \frac{120000m/60min}{0.4575m} = 72.86rad/se$$

Then calculate the angular speed "n"

$$n = \frac{60 * w}{2\pi} = \frac{60 * 72.86}{2\pi} = 695.76rev/min$$

Calculation of bearing load using equation (4.25 and 4.26)

$$P_1 = \left(0.625 + 0.0875\frac{h_1}{b}\right)M_1 g = \left(0.625 + 0.0875\frac{1.040}{0.978}\right)8500 * 9.81 = 59874.352N$$

$$P_2 = \left(0.625 - 0.0875\frac{h_1}{b}\right)M_1 g = \left(0.625 - 0.0875\frac{1.040}{0.978}\right)8500 * 9.81 = 44356.9N$$

Calculation of wheel force

$Y_1 = 0.35m_1g = 0.35 * 8500 * 9.81 = 29184.75N$

$Y_2 = 0.175m_1g = 0.175 * 8500 * 9.81 = 14592.375N$

Force on the axle (Force balancing the forces Y1 and Y2)

According to Table 4.5.

$H = \beta M1g = 0.175M1g$

$\beta = \frac{aq}{10} + fq$, Factor $\beta = 0.175$ comprises a quasi-static centrifugal Force percentage due to the unbalanced transverse acceleration a_q and a thrust factor f_q. The usual unbalanced transverse acceleration of $aq = 1\frac{m}{sec^2}$ results in a transverse force factor of 0.1(g, rounded up to $10\frac{m}{\text{sec}^2}$) to take into account the quasi-static centrifugal force.

It is evident that the unbalanced lateral acceleration a_q is given as:

$$a_q = \frac{V^2}{R}\cos^{-} - g\sin^{-} = \frac{V^2}{R}\cos^{-} - g\frac{P}{S}$$

Where v is vehicle speed, R (145m ERC) is curve radius and g = 9.81 m / s^2 is acceleration of gravity. Rail base (P) =162mm for UIC 54kg and tape line distance 2s (in case of standard-gauge rail vehicles, the tape line distance has a value of 2s = 1500 mm). The analysis an unbalanced transverse acceleration of $a_q = 1\frac{m}{\sec^2}$ was used.

According to tests of EN13104 led to a value being deprived of: Guiding axles $f_q = 0.07$!

$$H = Y_1 - Y_2 = 0.175 m_1 g = 0.175 * 8500 * 9.81 = 14592.375 N$$

Normal load on the wheel

$$Q_1 = \frac{\left[P_1(b+s) - P_2(b-s) + R(Y_1 - Y_2) - \sum_i F_i(2s - y_i)\right]}{2s}$$

$$Q_1 = \frac{\left[59870(0.978+0.75) - 44350(0.978-0.75) + 0.475(29185-14592) - \sum_i 4100(2*0.75-0.375)\right]}{2*0.75} = 34340N$$

$$Q_2 = \left[\frac{-p_1(b-s) + p_2(b+s) - R(Y_1 - Y_2) - \sum_i F_i y_i}{2*s}\right]$$

$$Q_2 = \left[\frac{-59870(0.978-0.75) + 44350(0.978+0.75) - 0.475(29185-14592) - \sum_i 4100*0.375}{2*0.75}\right] = 2590N$$

4.2.4 Gears

With gears, the theoretical tooth forces can be calculated from the power transmitted and the design characteristics of the gear teeth. Additional forces arising from the type and mode of operation of the machines coupled to the gear can only be determined when the operating conditions are known. Their influence on the rating life of the bearings is considered using an “operation” factor that takes shock loads and the efficiency of the gear into account. Values of this factor for different operating conditions can usually be found in information published by the gear manufacturer. The reactions between the mating teeth occur along the pressure line.

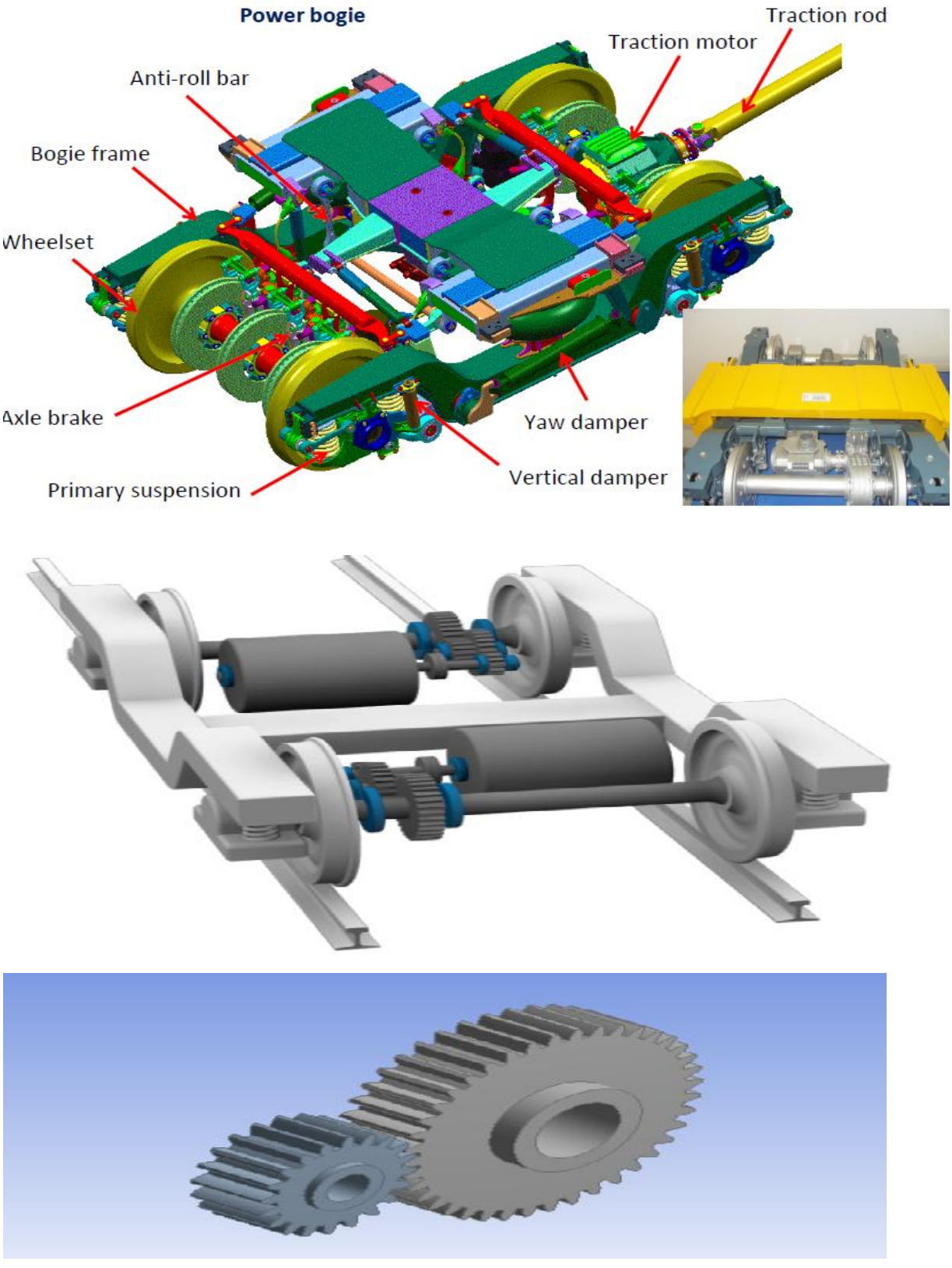

Fig bogie components 4.5

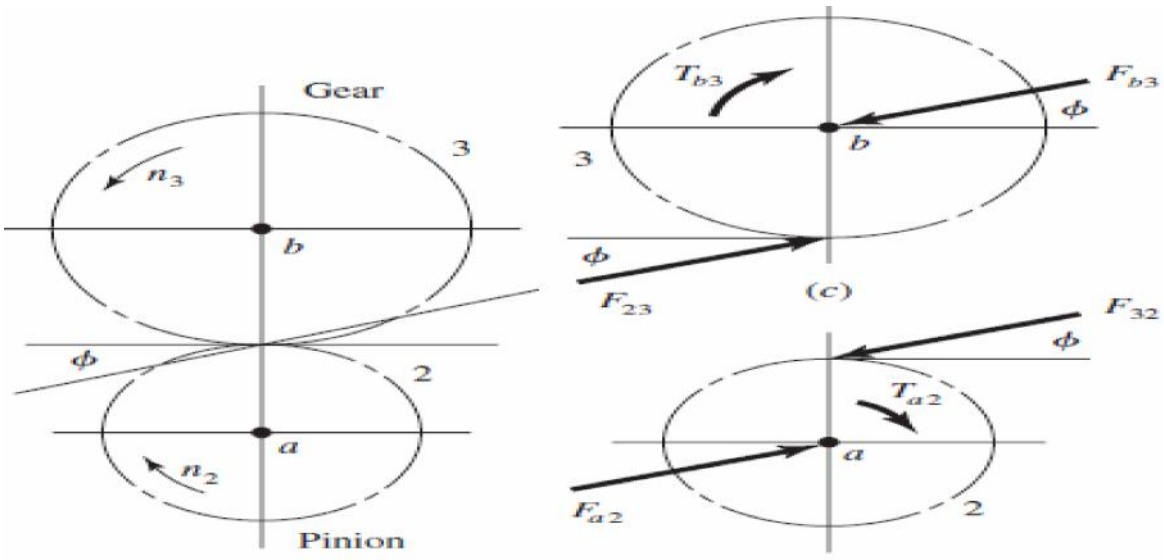

Figure 4-5Forces on gears

Force acting of traction motor forces on the pinion contact and the center of the rotor, in case of the traction motor shaft accommodating the pinion. Pinion mounted on shaft a motor axle rotating clockwise at n2 rev/min and driving a gear on shaft of railway axle at n3 rev/min. [Railway technical handbook Volume 2, page 16 and shigle 8 edition page 690-700]. To calculate forces on gears, the following relationship can be used:

We now define, W_t as the transmitted load. This tangential load is really the useful component, because the radial component serves no useful purpose. It does not transmit power. The applied torque and the transmitted load are seen to be related by the equation

$$T = \frac{P*60}{2®n} = \frac{120000*60}{2*®*406} = 2822.43Nm$$

$$F = \frac{2T}{d} = \frac{T}{r} = \frac{2822.43Nm}{0.2m} = 14112.13N$$

$$W_t = \frac{F}{\cos ¤} = \frac{14112.43}{\cos 20} = \frac{14112.13}{0.9397} = 15017.63N$$

where

$d = 400mm$

$Power = 120Kw$

$n = 406RPM$

$¤ = 20^0$

$T = torque$

4.3 Bending Moment between loading plane and running surface

The bending moment Mx in any section is calculated from forces P1, P2, Q1, Q2, Y1, Y2 and Fi as shown in Figure 4.4. It represents the most adverse condition for the axle, i.e.:

1) Asymmetric distribution of forces;

2) The direction of the forces Fi due to the masses of the unsprung components selected in such a manner that their effect on bending is added to that due to the vertical forces;

3) The value of the forces Fi results from multiplying the mass of each unsprung component by 1 g. The formulae to calculate Mx for each zone of the axle and the general outline of Mx variations along the axle.

Bending Moment Between loading plane and running surface:

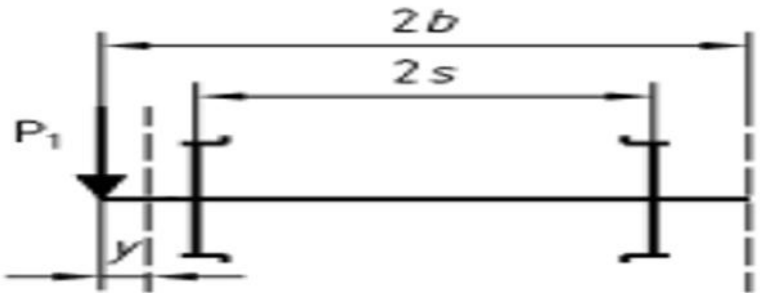

Figure 4-6bending moment b/n loading plane & running surface [EN 13103]

From this figure the shear force and bending moment is calculated as follows

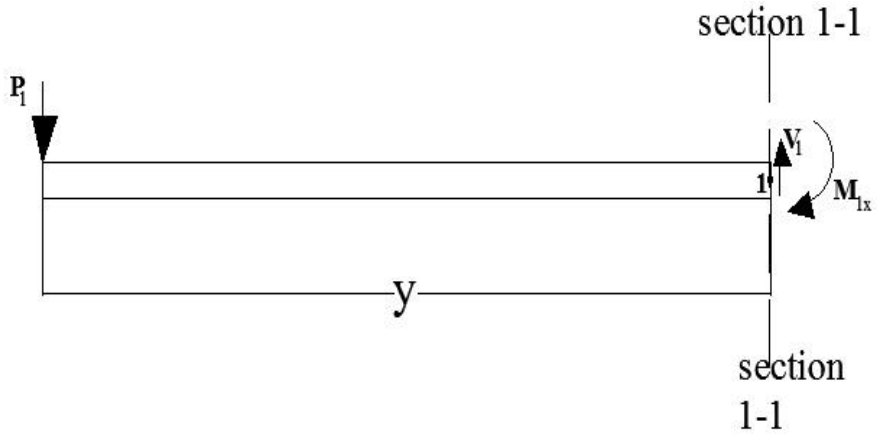

From equation 4.24 the value of P_1:

P_1=59874N

$$\sum Fv = 0$$
$$-P_1 + V_1 = 0$$
$$V_1 = P_1 = 59874N$$

$$\sum M_{1x} = 0$$

$$-P_1 y + M_{1x} = 0$$
$$M_{1x} = P_1 y$$

$$y = \frac{2b - 2s}{4} = \frac{1.96 - 1.5}{4} = 0.114m$$

$$M_{1x} = P_1 y = 59874 * 0.114 = 6825.64\ Nm$$

Bending moment between running plane and brake forces

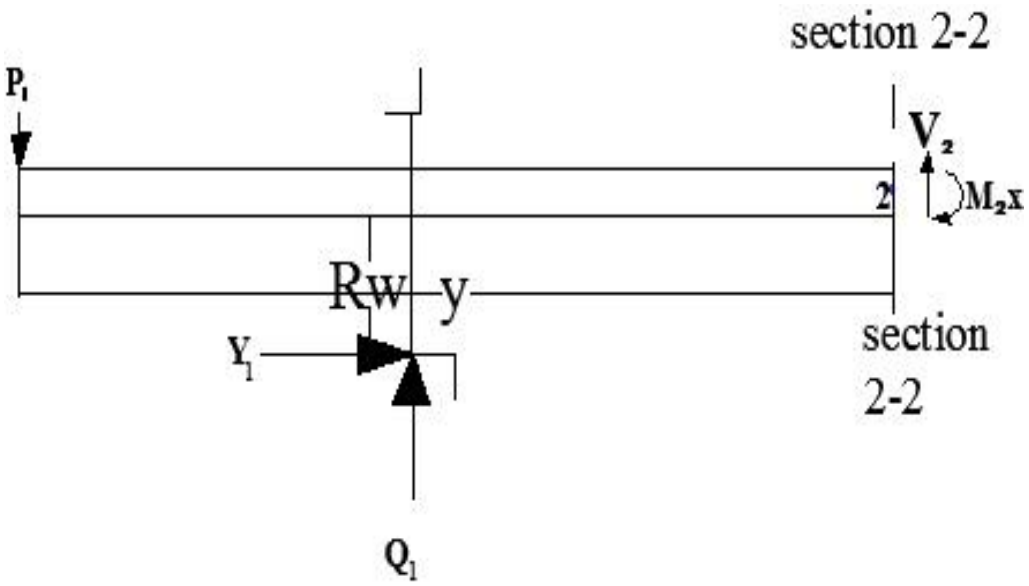

Where, y is a section distance

From the figure above (bending moment between running plane and brake forces), the shear force and bending moment calculated as follows.

$$\sum Fv = 0$$

From equation 4.25 and Table 4.5 the value of P_1 and Q_1 are=59874N, 34340N respectively.

$$-P_1 + Q_1 + V_2 = 0$$

$$V_2 = P_1 - Q_1$$

$$V_2 = 25534 \ \ N$$

$$\sum M_{2x} = 0$$

$$M_{2x} = P_1 y + Y_1 R - Q_1 \frac{yi}{2}$$

$$y = b - s + \frac{y_i}{2} = 0.978 - 0.750 + \frac{0.375}{2} = 0.4155m$$

$$R = 0.4575m$$

$$M_{2x} = 59874 * 0.4155 + 29184 * 0.4575 - 34340 * 0.1875 = 31790.6Nm$$

Bending Moment Between running surfaces

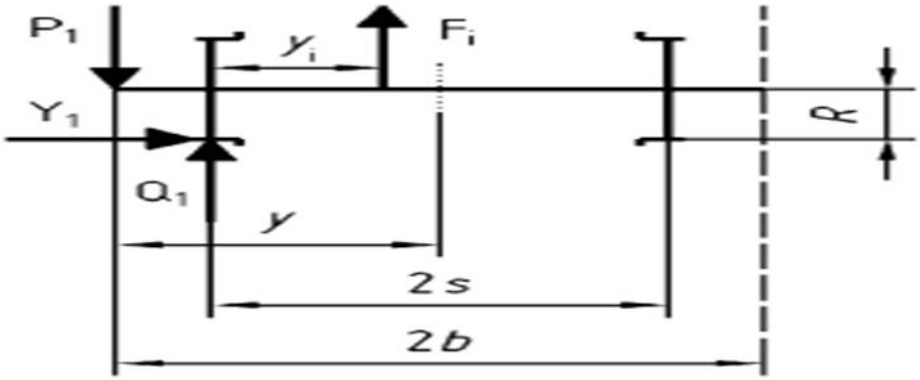

Figure 4-7Bending Moment Between running surfaces [EN 13103]

Fi: force(s) on the left of the section considered due to brake force.

From this figure the bending moment and shear forces are calculated as follows.

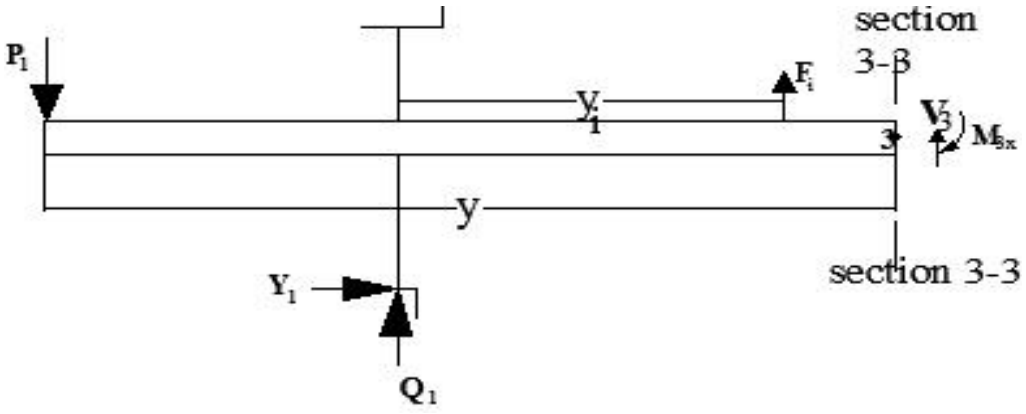

Where, y is a sectioning distance

From table 4.5 and equation 4.26 the value of P_1, Y1, Q1 and F_i are as follows:

P_1=59874N, Y1=29184N, Q1=34340N and F_i=41000N

$$\sum Fv = 0$$

$$-P_1 + F_i + Q_1 + V_3 = 0$$
$$V_3 = P_1 - (F_i + Q_1)$$
$$V_3 = 59874 - (41000 + 34340)$$
$$V_3 = 14334.065N$$

$$\sum M_{3x} = 0$$

$$M_{3x} = P_1\left(b - s + yi + \frac{s - yi}{2}\right) - Q_1\left(yi + \frac{s - yi}{2}\right) + Y_1R - Fi\left(\frac{s - yi}{2}\right)$$

$$M_{3x} = 59874 * 0.7905 - 34340 * 0.5625 + 29184 * 8 * 0.4575 - 41000 * 0.1875 = 336788Nm$$

4.4 Effects due to braking

Braking generates moments that can be represented by three components: M_x', My', $M_{z'}$.

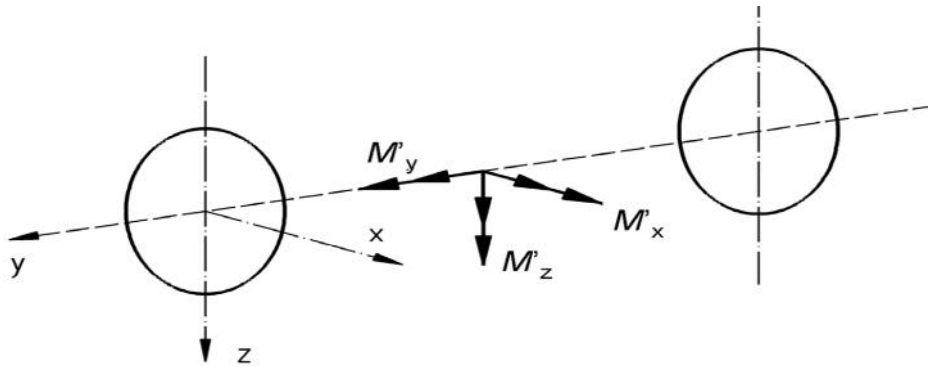

Figure 4-8Component of moments [EN 13103]

1. The bending component M_x' is due to the vertical forces parallel to the z axis.

2. The bending component M_z' is due to the horizontal forces parallel to the x axis.

3. The torsional component M_y' is directed along the axle centerline (y axis); it is due to the forces applied tangentially to the wheels. If several methods of braking are superimposed, the values corresponding to each method shall be added.

NOTE: If other methods of braking are used, the forces and moments to be taken into account can be obtained on the basis of the same principles. Special attention should be paid to the calculation of the M_x' component, which is to be added directly to the Mx component representing masses in motion.

4.4.1 Effects due to curving and wheel geometry

During curving the vehicle is guided by the forces between wheel and rail in the lateral direction. The vehicle is guided into the curve direction mainly by the lateral force on the flange of the outer leading wheel on each bogie. For an unbraked wheel set, the torsional moment M_y' is equal to 0.2 PR (20% of P*R if brake is not applied) to account for possible differences in wheel diameters and the effect of passing through curves. For a braked wheel set, these effects are included in the effects due to braking.

4.4.2 Method of braking used

Disc brakes use a clamping action to produce friction between the “rotor” and the “pads” mounted in the “caliper” attached to the suspension members. If right and left brakes have not the same effectiveness or right and left wheels have different radius of rolling circle, the axle has been subjected to additional torsional stress. However, for the case of lack of left and right symmetry, strength control is required for axial loads. Also, for the driving wheel sets due to UN symmetry of axle, axial wheel-rail forces cause moments and these moments form different bending stresses on axle.

Table 4-6 Data for calculating the Forces which work on the brake disc

[ADVANCED ENGINEERING 3(2009)1, ISSN 1846-5900]

Mass of the vehicle – M [kg]	70000
Start velocity – v_0 [m/s]	70
Deceleration – a [m/s^2]	1.4
Braking time – t_z [s]	50
radius of the braking disc – R_b[m]	0.250
Radius of the wheel – R_w [m]	0. 45750
Incline of the track – δ [‰]	11
Friction coefficient disc/pad – μ [/]	0. 35
Surface of the braking pad Ac – [mm^2]	20000
Brake seat distance(UIC)	375mm
Effective radius braking disc-r_d[m]	0.240

This heat ultimately transfers to the vehicle and the environment, and the disc cools down. To stop the wheel, braking pads are forced mechanically against the rotor or disc on both surfaces.

$$0.7*\frac{1}{2}*M*v_o^2 = \int_0^{t_z} P(t)dt = 2*F_{disc}\int_0^{t_z} V_{disc}(t)dt$$

They are compulsory for the safe operation of all vehicles. In short, brakes transform the kinetic energy of the vehicle into heat energy, thus slowing its speed. Brake fade is the reduction in stopping power that can occur after repeated or sustained application of brakes, especially in high load or high speed conditions. Brake fade is the reduction in stopping power that can occur after repeated or sustained application of brakes, especially in high load or high speed conditions. Brake fade can be a factor in any vehicle that utilizes a friction braking system. Brake fade is caused by a build-up of heat in the braking surfaces and the subsequent changes and reactions in the brake system components and can be experienced with both drum brakes

and disk brakes. Disc brakes are much more resistant to Brake fade because the heat can be vented away from the rotor and pads more easily, and became Steel construction has so many advantages: the strength to weight ratio is excellent, metals join easily, efficient shapes are available, etc. With those advantages, though, come some challenges that are best solved by a good understanding of how the metals actually perform in a structure.

The analysis is done by taking the distribution of braking torque between the front and rear axle is 70:30. Thus, Brake force on each front disc is as follows:

$$F_{disc} = \frac{0.7 * 0.5 * M * v_o^{\,2}}{2 * \frac{r_d}{R_w}(v_o * t_z - 0.5 * a * t_z^{\,2})} = 6276\ .30375\ \ N$$

Force determination for the brake caliper

Caliper disc brakes are among the most tried braking technologies in industrial use.

Designed to clamp onto both sides of discs or flat rails, these specialized brakes create friction that exerts a braking force on the disc attached to the rotating shaft, or on a rail or fin in linear motion applications. Caliper brakes are well suited for a range of industrial uses, such as construction machinery, material handling equipment, metalworking machinery, automated assembly machines, and o t h e r heavy equipment. The reactive force shifts the caliper housing and presses opposite side of braking pad against rotor. The surface pressure between the disc and the pad, on behave of the calculated force applied to the disc, needs to be determined.

The external pressure between the disc and the pads is calculated by the force applied to the disc.

$$P = \frac{F_{disc}}{A_c * «} = 0\ .8966 \quad (Mpa \quad)$$

Where Ac is the area surface of the pad in contact with the disc and μ the coefficient of friction.

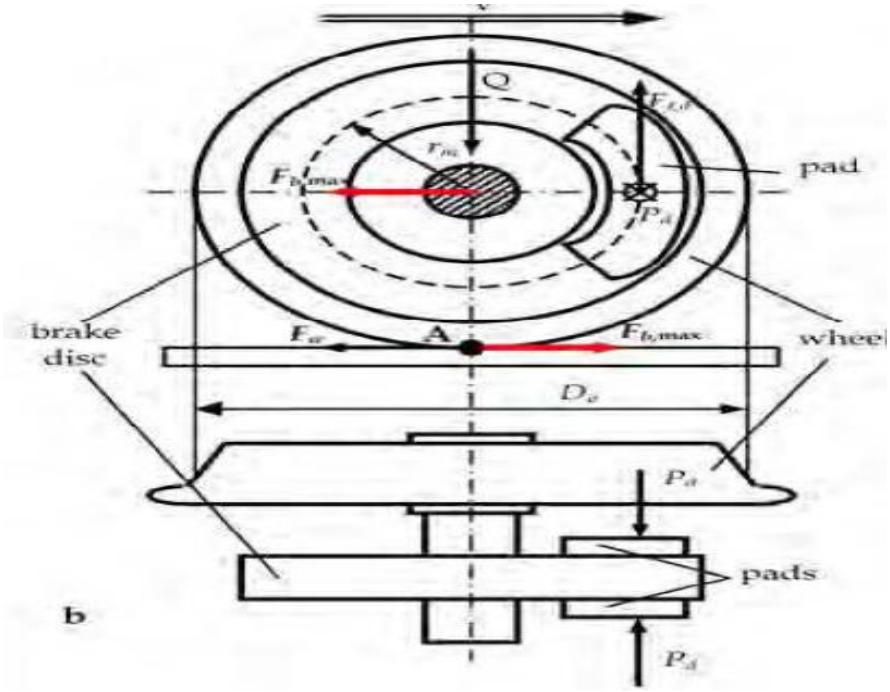

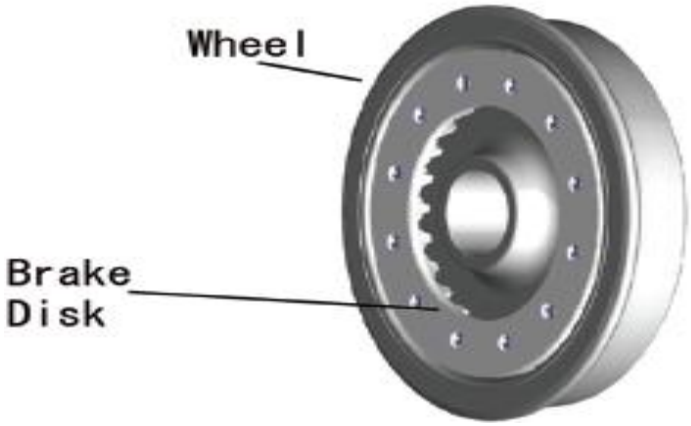

Fig 4.8.1 brake disc on railway axle

Bending Moment Determination by Braking Force

This is done by deteminening bending brake forces.

The braking force applied to axle is given by:

$$F_{bi} = \left(P_i S_i - F_{mi}\right)$$

Where:

- F_{bi} is the braking force applied on the axle;
- p_i is the pressure in the brake cylinder=360kpa
- Si is the cylinder surface=6000mm^2

- F_{mi} is the brake cylinder spring force=587.9N/mm^2
- τ is the brake rig ratio=0.9
- η is the brake efficiency=0.9
- μ is the brake friction coefficient=0.4
- ρ is wheel-rail adhesion coefficient, china standard for dry rail,

$$\circ = \frac{0.0624 + 45.6}{V + 260} = \frac{0.0624 + 45.6}{120 + 120} = 0.12016$$

Determine bending moment by brake force between loading planes and running surface

$$M_X' = F_{bi} \ll y = 9126 * 0.35 * 0.4155 = 1327 Nm$$

$$M_Z' = F_{bi} \ll \frac{Rb}{R} y = 91255 * 0.35 * \frac{0.250}{0.4575} * 0.4155 = 105242 Nm$$

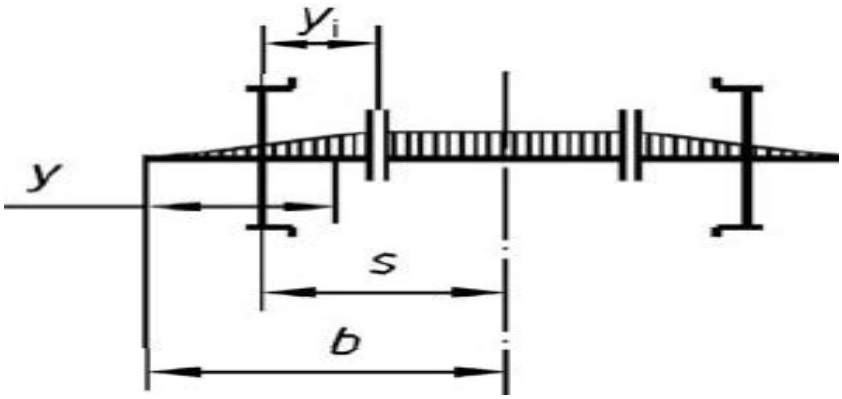

$$M_Y' = 0$$

Figure 4-9 braking moment between running surfaces and disc [EN 13103]

$$y = b - s + \frac{yi}{2}$$

$$y = 0.4155 \quad m$$

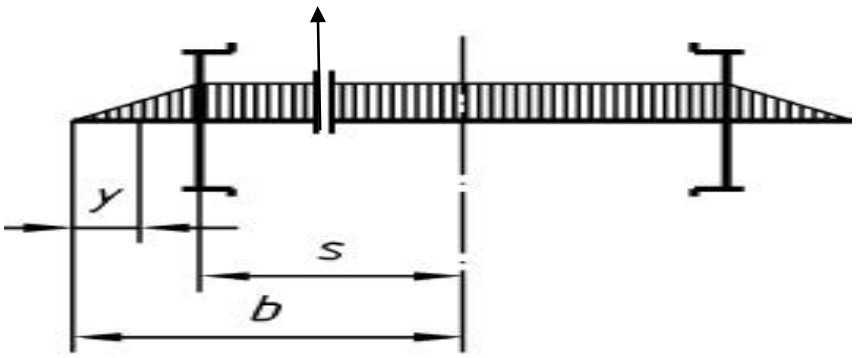

$$y = \frac{b-s}{2} + yi = 0.489m$$

Figure 4-10Braking moment between loading planes and running surface

$$M_X' = F_{bi} \ll (\frac{b-s}{2} + y_i) = 9126 * 0.35 * 0.489 = 1563Nm$$

$$M_Z' = F_{bi} \ll \frac{Rb}{R}(b-s) = 9125.5 * \frac{0.250}{0.4575}(0.78 - 0.750) = 397.4Nm$$

$M_Y' = 0.3P'R_w$ (Emergency brake distance on straight line (with 30% overload and with initial speed 120km/h) ≤800m)[ERC].

P': Proportion of P braked by any mechanical braking system (45%)

P: Half the vertical force per wheel set on the rail (M1+M2)/2) g

M_1: is mass of on journals (including bearings and axle boxes)

M_2: is mass of brake, gear (mass on wheel set between running surface)

Axle-box mass=1780kg

UN sprung-mass=1580kg

Sprung-mass=8500kg

$$P = \frac{(8500 + 1580 + 1780) * 9.81}{2} = 58114 \quad N$$

$$P' = 0.45 * P = 0.45 * 58114 = 26151 .3N$$

$$M_Y' = 0.3 * 26151 * 0.4575 = 3589 .2659 \quad Nm$$

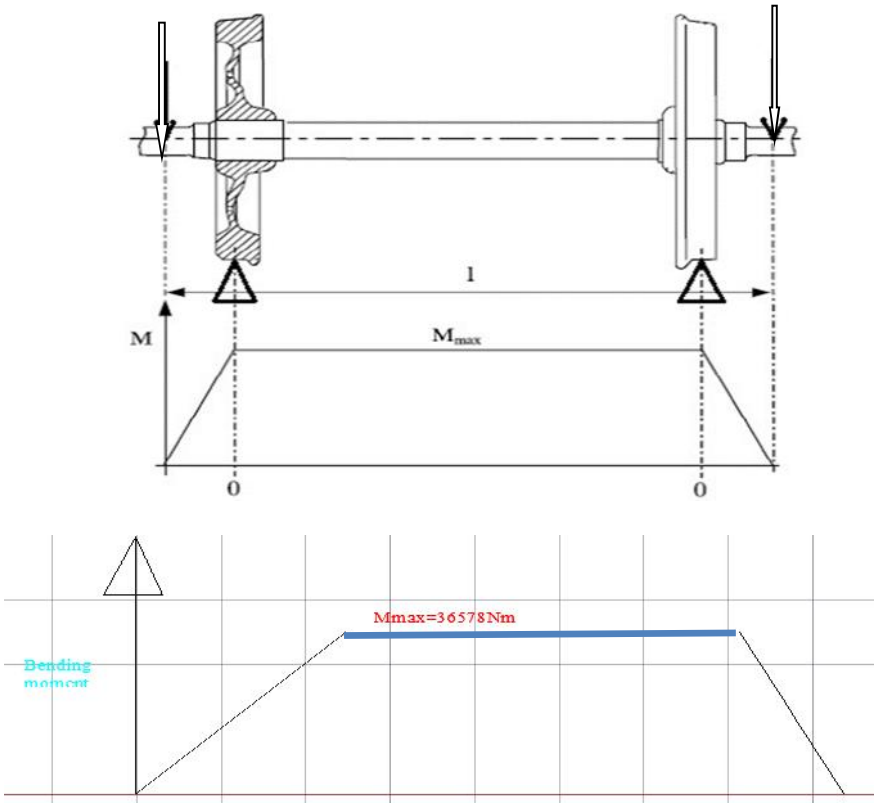

Figure 4 11loading and the consequent bending moment on the axle

Bending moment at different distance has the following expression:

$$M_b = [P_1 y, 0 < y < b - s]$$

$$M_b = \left[P_1 y - Q_1 \frac{y_i}{2} + Y_1 R_w, b - s < y < b - s + \frac{y_i}{2} \right]$$

$$M_b = \left[P_1 \left(b - s + y_i + \frac{s - y_i}{2} \right) - Q_1 \left(y_i + \frac{s - y_i}{2} \right) + Y_1 R_w - F_i \left(\frac{s - y_i}{2} \right), b - s + y_i < y < b - s + y_i + \frac{s - y_i}{2} \right]$$

[Railway vehicle handbook]

Due to P_1 is subjected to more heavenly side the bending moment increase up to zero on wheel seat and maximum at the center of the axle due to the effect of different component and decrease from maximum on less heavily side. Wheel seat is fixed support deflection and bending moment is zero.

4.4.3 Calculation of the resultant moment

In every section, the maximum stresses are calculated from the resultant moment MR which is equal to:

$MR=\sqrt{MX^2+MY^2+MZ^2}$, Where MX, MY and MZ are the sums of the various components due to masses in motion and braking:

$$MX = M_X + \sum M_X'$$

Where, M_x is total moment due to masses of vehicle

M_x' is bending moment due to brake force

$$MX = M_x + \sum M_x'$$
$$MX = Total$$
$$(MX)_1 = 6826 + 2888.83 = 9714.83Nm$$
$$(MX)_2 = 31790.6 + 2888.83 = 34679.43Nm$$
$$(MX)_3 = 33678.8 + 2888.8 = 36567.66Nm$$
$$MY = \sum M_y' = 3589.2659Nm$$
$$MZ = \sum M_z = 1052.424 + 397.6 = 1450.365Nm$$
$$MR = \sqrt{MX^2 + MY^2 + MZ^2} = 41174.4588Nm$$

NOTE: At a point on the outer surface of a solid cylinder with d as diameter, the components MX, MY and MZ generate:

A normal stress for MX and MZ;

A shear stress for MY.

The normal stress has the following value (bending of beams with a circular section):

$$\pm_n = \frac{32\sqrt{MX^2 + MZ^2}}{®d^3} = 44.9Mpa$$

The value of the shear stress is the following (torsion of beams with a circular section):

$$\pm_t = \frac{16MY}{®d^3} = 3Mpa$$

As a result, the two principal stresses σ_1 and σ_2 are obtained as:

$$\pm_1 = \frac{\pm_n + \sqrt{\pm_n^2 + 4\pm_t^2}}{2} = 45.1Mpa$$

$$\pm_2 = \frac{\pm_n - \sqrt{\pm_n^{\,2} + 4\pm_t^{\,2}}}{2} = -0.2Mpa$$

$$\sigma = \sigma_1 - \sigma_2 = \sqrt{\sigma_n^{\,2} + 4\sigma_t^{\,2}} = \frac{32}{\pi d^3}\sqrt{MX^2 + MY^2 + mZ^2} = 45Mpa$$

Starting with point "left side"

$$M_a = \frac{Mb_{\max} - Mb_{\min}}{2}$$

$$Ma = \frac{36567 - 3589}{2} = 16488.87\,Nm$$

M_a=16488.87Nm

$$T_a = \frac{8500 * 9.81 * 0.915}{2} = 38108.784\,Nm$$

From Table 4.2

We are selecting a material of AISI 1050

σ_{ut} = 655Mpa

σ_y = 515Mpa

The Endurance Limit

From shigley 8 edition page 281, for steels, we will estimate the endurance

Limit as $\pm_e = 0.5\pm_{ut}, \pm_{ut} \le 200kpsi(1400Mpa)$

$\sigma'_e = 0.5 * \sigma_{ut} = 0.5 * 655\text{Mpa} = 327.54\text{Mpa}$

From (shigley 8 edition page 287, table 6.2) the value of a and b is given below:

Machine cold drawn

$k_a = a\sigma_{ut}^{b}$

a=4.51

b=-0.265

$k_a = a\sigma_{ut}{}^{b} = 4.51 * (655 * 10^6)^{-0.265} = 0.8288$

Size factor, k_b

From shigley 8 edition page 287

$$K_b = \{(1.51d^{-0.107}), 51 < d \le 254mm$$

$$k_b = 1.51(210)^{-0.107}$$

$$k_b = 0.8$$

Loading Factor, k_c

When fatigue tests are carried out with rotating bending, axial (push-pull), and torsional loading, the endurance limits differ with $\pm_{ut}$. From shigley page 289, $k_c = 1$ because the axle is subjected to rotating bending.

Temperature Factor, k_d : When operating temperatures are below room temperature, brittle fracture is a strong possibility and should be investigated first. When the operating temperatures are higher than room temperature, yielding should be investigated first because the yield strength drops off so rapidly with temperature.

$$k_d = 0.975 + 0.432(10^{-3})T_F - 0.115(10^{-5})T_F{}^2 + 0.104(10^{-8})T_F{}^3 - 0.595(10^{-12})T_F{}^4$$

Where $70 \le TF \le 1000$◦F.for this analysis take 98TF

$$k_d = 1.007$$

Reliability Factor, k_e : Where the mean endurance limit is shown to be $\frac{S_e'}{\pm_{ut}} = 0.5$

, thus the reliability modification factor to account for this can be written as

$k_e = 1 - 0.08 z_a$: From shigley 8 edition page 292 table 6.5 at 50% reliability, the transformation variant (z_a) is zero then $k_e = 1 - 0.08(0) = 1$

$$S_e = k_a k_b k_c k_d k_e \sigma'_e = 0.8288 * 0.8 * 327.54\text{Mpa} = 217.1456\text{Mpa}$$

For the standard shoulder fillet, for estimating k_t values for the first iteration, an r/d ratio should be selected so k_t values can be obtained.

Assume that $k_t = 2.7, k_{ts} = 2.2$and $k_t = k_f, k_{ts} = k_{fs}$for a shoulder fillet-shoulder ($0.02 = \frac{r}{d}$)

DE-Goodman

$$d = \left(\frac{16}{\pi}\left\{\frac{1}{S_e}\left[4(f_f M_a)^2 + 3(K_{fs}T_a)^2\right]^{1/2} + \frac{1}{S_{ut}}\left[4(K_f M_m)^2 + 3(K_{fs}T_m)^2\right]^{1/2}\right\}\right)^{1/3}$$

$T_a=0$ and $M_m=0$

$$d = \left(\frac{16}{\pi}\left\{\frac{1}{217.98 * 10^6}\left[4(2.7 * 16414)^2\right]^{1/2} + \frac{1}{655 * 10^6}\left[3(2.2 * 38108.643)^2\right]^{1/2}\right\}\right)^{1/3}$$

$$= 0.1747\text{m}$$

From the standard size of shaft

d=175mm

Typical $1.2 = \frac{D}{d} \rightarrow D = 1.2 * d = 1.2 * 175\text{mm} = 210\text{mm}$

There is a significant variation in typical bearings in the ratio of fillet radius versus bore diameter, with r/d typically ranging from around 0.02 to 0.06.

$0.02 = \frac{r}{d} \rightarrow r = 0.02 * d = 0.02 * 175\text{mm} = 3.5\text{mm}$

From the standard table shigle Design books

$k_t = 2.6, k_{ts} = 1.9, q = 0.8$ and $q_s = 0.8$

$k_f = 1 + q\ k_t - 1 = 1 + 0.8\ 2.6 - 1 = 2.28$

$$k_{ft} = 1 + q_s\ k_{ts} - 1 = 1 + 0.8\ 1.9 - 1 = 1.81$$

$k_b = 1.51175^{-0.157} = 0.671$

$k_b = 0.8288$

$S_e = k_a k_b k_c k_d k_e \sigma'_e = 0.8288 * 0.671 * 374\text{Mpa} = 120.802\text{Mpa}$

$\sigma'_a = (\sigma_a^2 + 3\tau_a^2)^{1/2} = [(32k_f m_a/\pi d^3)^2 + 3(16k_{fs}T_a/\pi d^3)^2]^{1/2}$

Where:-$T_a = 0$

$\sigma'_a = (\sigma_a^2 + 3\tau_a^2)^{1/2} = [(32k_f m_a/\pi d^3)^2]^{1/2} = \frac{32 * 2.28 * 16414}{\pi(0.175)^3} = 71.14\text{Ma}$

$\sigma'_m = (\sigma_m^2 + 3\tau_m^2)^{1/2} = [(32k_f m_m/\pi d^3)^2 + 3(16k_{fs}T_m/\pi d^3)^2]^{1/2}$

Where $M_m = 0$

$$\sigma'_m = (\sigma_m^2 + 3\tau_m^2)^{1/2} = [3(16k_{fs}T_m/\pi d^3)^2]^{1/2}$$
$$= [3(16 * 1.81 * 38108/\pi(0.175)^3)^2]^{1/2} = 113.78\text{Mpa}$$

Calculate factor of safety as follows

$$\frac{1}{n_f} = \frac{\sigma'_a}{S_e} + \frac{\sigma'_m}{S_{ut}} = \frac{71.14}{120.802} + \frac{113.78}{655} = 0.76328699 \rightarrow n_f = 1.396534$$

$n_f = 1.4$ So that it is safe

From standard table the hub diameter of a wheel (D= 915mm) for which is much with d=177+-3mm.

To find Number of Cycles

$$S_f = \frac{\sigma_a * \sigma_{ut}}{\sigma_{ut} - \sigma_m}$$

$\sigma_{ut} = 655 \; Mpa$

$\sigma_a = 71.14 \; Mpa$

$\sigma_m = 113.9 \; Mpa$

$$f = \frac{\sigma_f' (2 * 10^3)^b}{\sigma_{ut}}$$

$\sigma_f' = \sigma_{ut} + 345 \; Mpa$

$$f = \frac{1000 \; (2000)^b}{655} = 0.9$$

$$b = \frac{-\log\left(\frac{\sigma_f}{Se'}\right)}{\log(2Ne)} = \frac{-\log\left(\frac{1000}{327.5}\right)}{\log(2000000)}$$

$$S_f = \frac{71.14 * 655}{655 - 113.9}$$

$S_f = 86.1006289 \; Mpa$

$fS_{ut} = 0.9 \; S_{ut} = 0.9 * 655 = 589.5 \; Mpa$

$\log(0.9 \; S_{ut}) = \log(589.52 \; Mpa) = 2.773$

$\log(Se) = \log(120.802) = 2.0832$

$\log(S_f) = \log(86.1009) = 1.9123$

$$Therefore, \quad \log(N) = \frac{(6 - 1)(2.773 - 1.9123)}{(2.773 - 2.0832)} = 6.2173$$

$N = 1.65 * 10^6 \; cycles$

4.5 Bearing selection

Bearings are designed to meet certain requirements, usually expressed in terms of load carrying capacity, stiffness, and dynamic behavior. Many of these properties are quantified, but good design also involves several nonmathematical variables, such as how the lubricant

is applied, how to accommodate misalignment, and what to do about starting and stopping a bearing.

4.5.1 Characteristics of Axle Bearings

Rolling stock axle bearings are subject to radial impact loads caused by rail joints, switches and sometimes wheel flats, as well as to the static and dynamic radial loads of vehicle weight. They are also liable to receive axial loads generated by lateral movement as trains run on curved rails or in a snaking motion. All of these loads together form complex combinations that act on axle bearings. Axle bearings must therefore be designed on the basis of not only dimensional requirements of the axle journal and bearing box geometry, but also these complex load conditions. Additionally, as axle bearings play a critical role in the safety of railroad operation, they are periodically disassembled for inspection. Bearings are manufactured to take pure radial loads, pure thrust loads, or a combination of the two kinds of loads.

4.5.2 Journal Bearings

Train passenger's safety depends on the reliability and durability of journal bearings. Journal bearings are generally characterized by larger width and smaller radius and can be cylindrical roller bearing type, tapered roller bearing type or self-aligning roller bearing type. Ball bearings are used to support thrust loads. Also, ball bearings could be used as journal bearings in lightly loaded applications. A bearing or bearing assembly on a rail vehicle axle journal that transmits a proportion of the weight of the rail vehicle directly to the wheel set. For the purpose of this definition bearings associated with the mounting of traction motors or traction drives are excluded.

4.5.3 Cylindrical Roller Bearings

Cylindrical roller bearings (CRBs) have high load-carrying capacity because of the linear contact between their rollers and raceways. They are capable of high running speeds because of their relatively small friction coefficient and they offer advantages in maintenance because they are more easily disassembled, inspected and reassembled. Furthermore, they allow the free setup of their axial clearance. However, ordinary CRBs require another bearing to handle axial loads, increasing the number of parts required for supporting the axle journal.

Double or Four Row Cylindrical Roller Bearings: It is fitted with a ball bearing on the axle end for thrust load support. The axle end side of the ball bearing is sometimes fitted with coned disc spring or rubber buffers to absorb shock loads.

Double Row Cylindrical Roller Bearings (with Ribs): This bearing supports thrust loads with its inner and outer ring rib side faces. Since a ball bearing is not needed for thrust loading, this design is more reasonably priced. It is popular for its high grease fill and durability.

4.6 Axle box

Axle boxes are the linking design element between the rotating wheel set and the quasi-static frame of the bogie or running gear of a railway vehicle. All forces acting between these components are transmitted via springs, dampers and guiding elements. Axle boxes and axle box bearings/units have always been a vital component in the reliability of railway rolling stock and they have a considerable influence on the operating safety, reliability and economics of railways. Select typical two-piece link arm design because of our bogie configuration, number of Axle, total load in addition to this very reliable and less maintenance cost. A structure, including for example a cartridge bearing adaptor, which houses, or is in contact with, the axle journal bearing and provides an interface with the bogie and / or suspension arrangement.

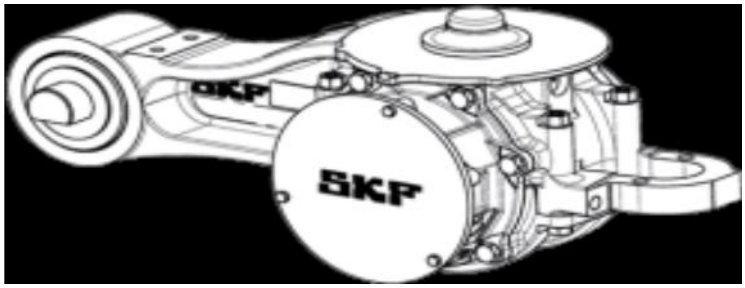

Figure 4-11 Typical two-piece link arm [17]

4.7 Lubrication

The primary objective in lubrication is to reduce the severity of both the normal and shear stresses in solid surface contact. The region of contact between the wheel hub and axle was at the bottom of the axle, which is where lubricant settled. Railroad car axles, by contrast, rotate in stationary bearings [journals] where the contact region is at the top of the axle.

Lubricants used in mechanical application have several important tasks [Sch10-2]:

Transmission of forces due to hydrodynamic thin films and physical or chemical Induced reaction films .Removing of chips and cooling effects when used as cooling lubricant in metalworking In most mechanical systems (transport, energy production, manufacturing), lubricants are used to reduce friction and wear between moving parts. Lubricants are composed of base oils and additions named additives or active substances. Despite continuous improvements of base oils the relevance of high performing additive packages increases due to increasing demands. Thereby, the interaction of a large number of different additives contained in the oils and the lubricated surfaces plays an important role. The additive package will nearly always contain anti wear additives, metal-containing detergents (e.g. salicylates, sulphonates), and ash less dispersants. In each of these classes of additives, the formulator may use a mixture of two or more components to achieve the desired performance profile. Supplementary additives such as antioxidants or friction modifiers may also be present. [Pir02] The main focus of this paragraph lies on the interaction of lubricant additives with metal surfaces and the formation of tribo-reactive thin films. Further information about the composition of lubricants and the mode of action of selected additives can be found for example in [Man07].

4.7.1 Lubrication regimes

The thickness of fluid films in tribological lubricated contacts determines the lubrication regime or rather the type of lubrication. Commonly accepted are three basic lubrication regimes. The distinction is based on different domains of the Stribeck curve, describing the evolution of the coefficient of friction over the ratio λ of lubricant film thickness to roughness ratio. The λ ratio is often simply known as Tallian pa*rameter.

Hydrodynamic lubrication valid for $\lambda > 3$ – two surfaces are completely separated by a fluid film. There are two conditions for the occurrence of hydrodynamic lubrication: Two surfaces must move relatively to each other with sufficient velocity for a load carrying lubricating film to be generated and, Surfaces must be inclined at some angle to each other, i.e. if the surfaces are parallel a pressure field will not form in the lubricating film to support the required load.

Hydrodynamic lubrication is only effective when an appreciable sliding velocity exists. A sliding velocity of 1 [m/s] is typical of many bearings. As the sliding velocity is reduced the film thickness also declines to maintain the pressure field. This process is very effective as pressure magnitudes are proportional to the square of the reciprocal of film thickness.

Eventually though the film thickness will have diminished to such a level that the small high points or asperities on each surface will come into contact. Contact between asperities causes wear and elevated friction. Mixed/boundary lubrication valid for $1 < \lambda < 3$ – two surfaces are partly separated or partly in contact. Provide full separation of the contacting surfaces. As a result of that, direct contact between the highest asperities takes place which may lead to accelerated running-in. The magnitude of the frictional force and the rate of wear are significantly lower than in the case of boundary lubrication.

Boundary lubrication valid for $\lambda < 1$ – two surfaces are mostly in contact with each $'^{a}U'$ other even though a fluid is present. Furthermore the surface topography or even surface texture, which refers to the arrangement or orientation of roughness, affects the lubricant film thickness. In case of EHD (elastohydrodynamic) or fully fluid contacts, the surface topography plays no decisive role due to the total separation of the facing surfaces. The surface texture has no influence as the λ ratio is high. However, as the facing surfaces are getting closer, the roughness values may play a role as the lubricant has a certain relaxation constant. The lubricant will not flow in the same way, if the texture is oriented in motion direction, or if it is transversal.

4.7.2 Lubrication Selection

Gear and axle lubricants promote temperature reduction via friction reduction. In addition, they must maintain appropriate viscosity at both high and low temperatures, and must remain stable over long periods of time. The contacting surfaces in rolling bearings have a relative motion that is both rolling and sliding, and so it is difficult to understand exactly what happens. If the relative velocity of the sliding surfaces is high enough, then the lubricant action is hydrodynamic. Elastohydrodynamic lubrication (EHD) is the phenomenon that occurs when a lubricant is introduced between surfaces that are in pure rolling contact. When a lubricant is trapped between two surfaces in rolling contact, a tremendous increase in the pressure within the lubricant film occurs. But viscosity is exponentially related to pressure, and so a very large increase in viscosity occurs in the lubricant that is trapped between the surfaces. The purposes of an antifriction-bearing lubricant may be summarized as follows:

- To provide a film of lubricant between the sliding and rolling surfaces
- To help distribute and dissipate heat
- To prevent corrosion of the bearing surfaces
- To protect the parts from the entrance of foreign matter

Chapter 5.

AXLE ANALYSIS WITH ANSYS SOFTWARE AND RESULTS

Before going to the finite element analysis, the modeling of the axle should be made. The figure given below shows the model of the axle and its component made in CATIA V5R16 window. Structure parts are made with the real profiles and Finite element modelling is made with ANSYS 12 Workbench. The structure model made by CATIA V5R16 software is imported to ANSYS 12 workbench. In order to import the CATIA made model to ANSYS 12 window, both software's run at the same time. The model in CATIA is opened. Then with the import option found in ANSYS workbench, the modelling is imported.

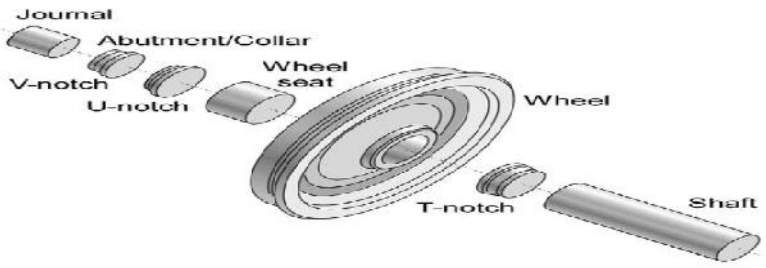

Figure 4-12Schematic drawing of various section of a railway axle by CATIA V5R16.

The typical geometries for these regions (named as T-notch, U-notch, V-notch and S-transition) are described. Considering the typical T and U notches, two FEM models have been built on the basis of the axle diameters of 210 and 177 mm, while the S-transition (transition between wheel and disk seats) has been modelled as the merging of two adjacent Transitions with a minimum diameter of 144 mm. Stress concentration factor – K_t – is in the range 1.15-2.6.

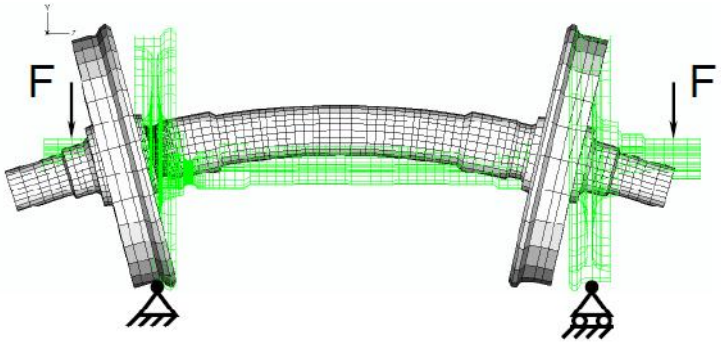

Figure 4-13whole model with applied vertical forces

The bending moment was applied as two vertical load located at bearing centers as shown in the above figure.

5.1 Finite Element Analysis of Locomotive Axle

Due to the complex structure, only reasonable simplified model can make it possible to describe mechanical characteristics of the overall structure. Finite element model of axle was established to do the strength calculation. In this way, stress distribution can also be obtained. In the process of modeling, element type of each part should be decided in the first place. The selection of element with regular shape and fewer nodes should be based on the precision requirement. The reason for reducing the total number of nodes as many as possible is to effectively decrease the cost. As the difference of steel types, strength of different part is quite different. Steel elastic modulus is 205GPa, Poisson's ratio is 0.290 and density is 7850 kg/m^3 is used in this FEM (ANSYS) analysis.

5.2 Fatigue Results In ANSYS Workbench

In ANSYS Workbench, there are nine results for evaluating fatigue is available for the user. These are,

1. Life:-This result contour plot shows the available life for the given fatigue analysis. If loading is of constant amplitude, this represents the number of cycles until the part will fail due to fatigue. If loading is non-constant, this represents the number of loading blocks until failure. Thus if the given load history represents one month of loading and the life was found to be 120, the expected model life would be 120 months. In a constant amplitude analysis, if the alternating stress is lower than the lowest alternating stress defined in the S-N curve, the life at that point will be used.

2. Damage:-Fatigue damage is defined as the design life divided by the available life. The default design life may be set through the options dialog box. A damage of greater than 1 indicates the part will fail from fatigue before the design life is reached.

3. Safety Factor: - This result is a contour plot of the factor of safety (FS) with respect to a fatigue failure at a given design life. The maximum FS reported is 15. For Fatigue Safety Factor, values less than one indicate failure before the design life has been reached.

4. Biaxiality Indication: - Biaxiality indication is defined as the smaller in magnitude principal stress divided by the larger principal stress with the principal stress nearest zero

ignored. This result is a stress biaxiality contour plot over the model that gives a qualitative measure of the stress state throughout the body. A biaxiality of 0 corresponds to uniaxial stress, a value of -1 corresponds to pure shear, and a value of 1 corresponds to a pure biaxial state. Fatigue material properties are typically based on uniaxial stresses. Real world stress states are usually multiaxial. This fatigue result gives the user some indication of the stress state over the model and how to interpret the results. For Non-proportional loading, you can choose between average biaxiality and standard deviation of biaxiality in the Details view.

5. Equivalent Alternating Stress:-The Equivalent Alternating Stress contour is the stress used to query the S-N curve. This result is not valid if the loading has non-constant amplitude (Loading Type = history data). The result is useful for cases where the design criterion is based on an equivalent alternating stress as specified by the fatigue analyst. Equivalent alternating stress is the last calculated quantity before determining the fatigue life. “Equivalent alternating stress” is the stress used to query the fatigue SN curve after accounting for fatigue loading type, mean stress effects, multiaxial effects, and any other factors in the fatigue analysis. This result is not applicable to Stress life with non- constant amplitude fatigue loading due to the fact multiple SN queries per location are required and thus no single equivalent alternating stress exists.

6. Rain flow Matrix (history data only):-This graph depicts how many cycle counts each bin contains. This is reported at the point in the specified scope with the greatest damage. Shows the rain flow matrix at the critical location. Only applicable for non-constant amplitude loading where rain flow counting is needed. This result may be scoped.

7. Damage Matrix (history data only):-Similar to the rain flow matrix, this graph depicts how much relative damage each bin has caused. This result can give you information related to the accumulation of the total damage (such as if the damage occurred though many small stress reversals or several large ones). Shows the damage matrix at the critical location on the model. This result is only applicable for non-constant amplitude loading where rain flow counting is needed. Z-axis corresponds to the percent damage that each of the Rain flow bin’s cause. Similar to the rain flow matrix except that the percent damage that each of the Rain flow bin’s cause is plotted on the Z-axis. This result gives the user a measure of the composition of what is causing the most damage.

8. Fatigue Sensitivity:-This plot shows how the fatigue results change as a function of the loading at the critical location on the scoped region. Sensitivity may be found for life,

damage, or factory of safety. For instance, if you set the lower and upper fatigue sensitivity limits to 50% and 150% respectively, and your scale factor to 3, this result will plot the data points along a scale ranging from a 1.5 to a 4.5 scale factor. You can specify the number of fill points in the curve, as well as choose from several chart viewing options (such as linear or log-log). Shows how the fatigue results change with loading at the critical location on the model. User specifies: Sensitivity for life, damage, or factor of safety, Number of fill points, Load variation limits.

9. Hysteresis:-In a strain-life fatigue analysis, although the finite element response may be linear, the local elastic/plastic response may not be linear. The Neuber correction is used to determine the local elastic/plastic response given a linear elastic input. Repeated loading will form close hysteresis loops as a result of this nonlinear local response. In a constant amplitude analysis a single hysteresis loop is created although numerous loops may be created via rain flow counting in a non-constant amplitude analysis. The Hysteresis result plots the local elastic-plastic response at the critical location of the scoped result (the Hysteresis result can be scoped, similar to all result items). Hysteresis is a good result to help you understand the true local response that may not be easy to infer.

Define Structural Analysis: Structural analysis is used to determine deformation, stain, stress and other structural analysis. Static structural analysis is performed in ANSYS work bench.

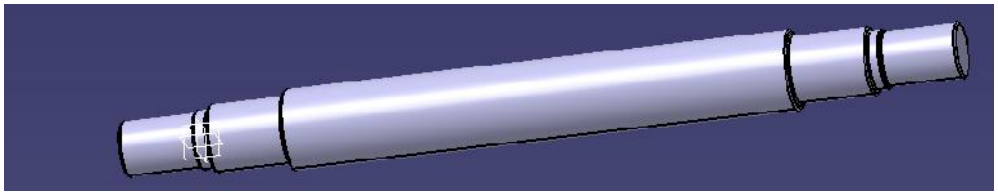

Figure 4-14 3D-axle modelling By CATIA V5R16

Boundary Conditions and Material Properties (FEM Modelling)

The model was meshed; the loading and boundary conditions were applied and the finite element linear elastic stress analysis was performed by using the ANSYS. A three dimensional model of axle is imported to static structural workbench of ANSYS, various loading and boundary conditions are applied on it. Material properties of Carbon Steel are considered. During analysis two boundary conditions has been considered which on railway axle are as follows: Fixed support at the one side axle and other side axle wheel seat.

5.3 Axle meshing

During analysis default meshing is taken in ANSYS 12.Then meshing of model has been done using default meshing type. Meshing is an important part of Finite Element modeling which has a strong influence on the reliability and accuracy of results as well as the model efficiency. Refined mesh usually provides more accurate results than coarse mesh. However the refined mesh increases the computational cost significantly. Hence, some meshing strategies are employed to set up a reliable Finite Element model with reasonable cost. For the parts which undergo high level loading or stress, refined mesh is necessary. On the other hand, for the parts which are away from the severe loading or stress condition, coarse mesh is suitable to reduce the model size. After completion of meshing we apply forces at various section of the axle with fixed support at wheel seat. Bearing seat and disc brakes are refined mesh because of high load act on it.

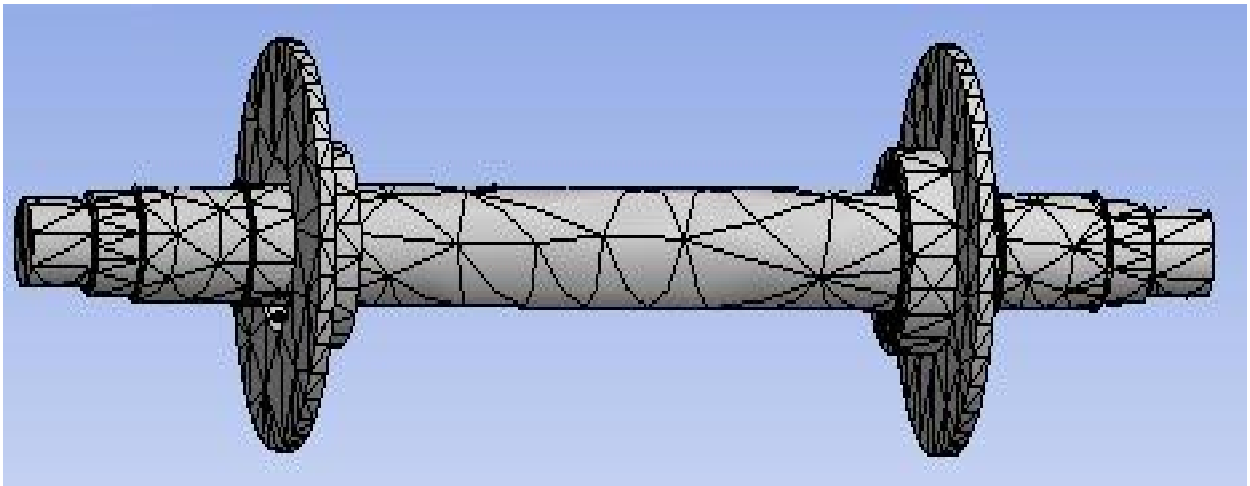

Figure 4-15Axle meshing

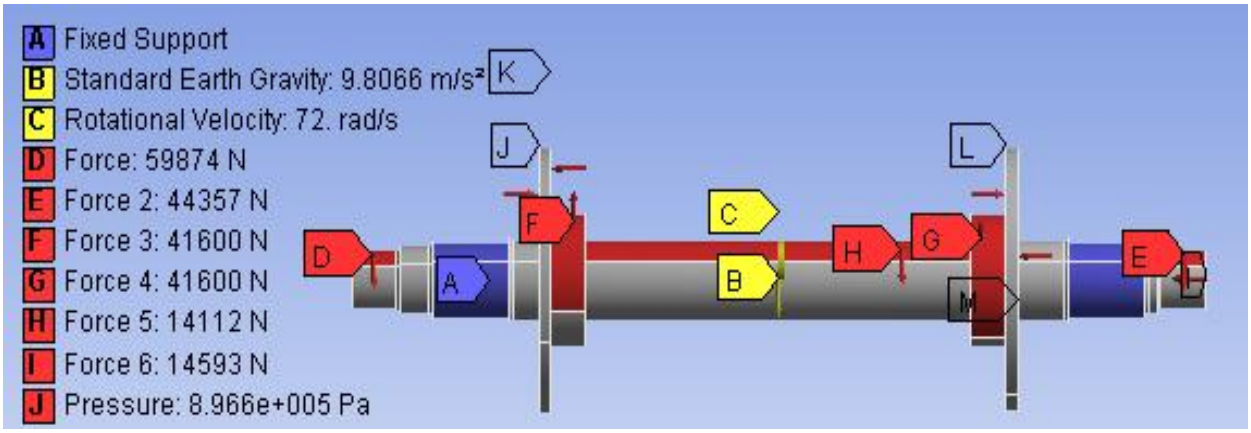

Figure 4-16Load application on the Axle

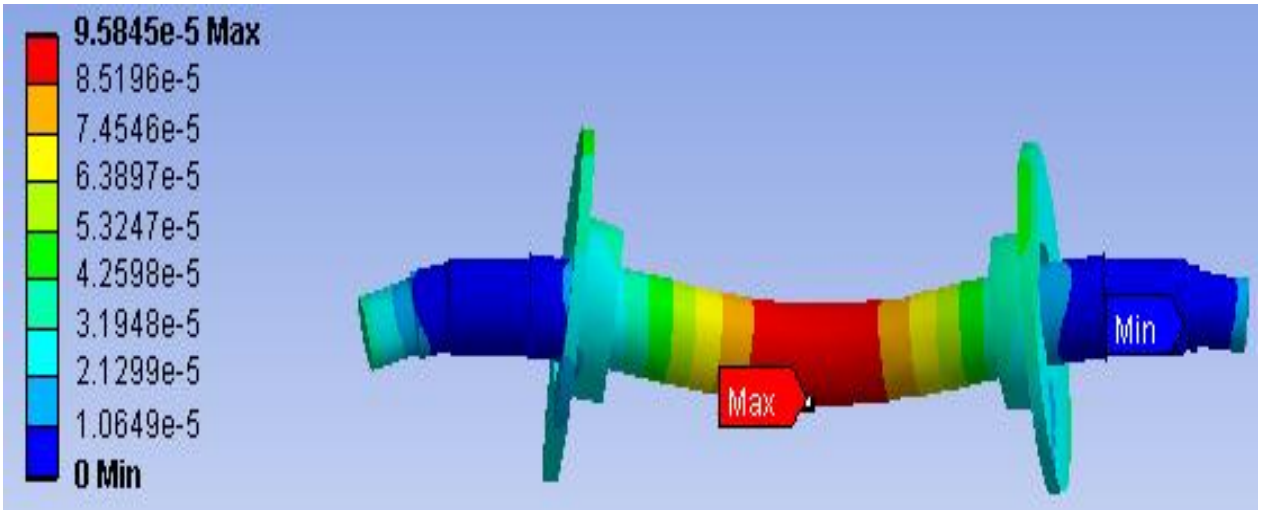

Figure 4-17Total deformation

The total deformation of the axle is maximum 0.00009581mm due to the effect of different components such as brakes ,gears ,calipers at the body of the axle and minimum =0 at the wheel seat due to fixed support. Deformation is maximum at on brake disc due to high pressure of caliper on pads of the axle because of brake force and lateral forces act on it through axle. The sectional view shows that no damage occurs in the interior of the axle so that it is safe.

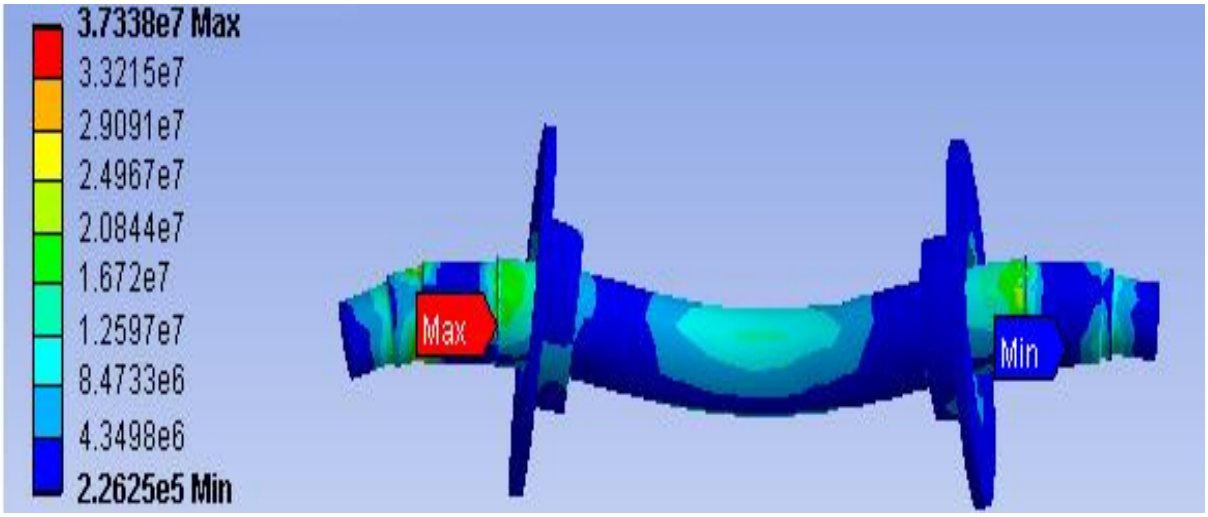

Figure 4-18Equivalent (von-Mises) stress

A comparison of the value of maximum Von-Mises stress with the material yield strength (presented in Table 4.2) revealed that the material strength is many times larger than the maximum stress demonstrating no plastic deformation in the axle. The position of the maximum stress (those locations experience high local stresses due to concentrated loads

applied). Fig. 5.7 shows clearly that the maximum Von-Mises stress of about 37.338Mpa MPa occurs on the axle surface at the first fillet near to the bearings location. Von-mises stress is maximum at stress concentration or when change in diameters occurred. The shape of a component or structure and boundary conditions dictates how it will respond to service loads in terms of stresses, strains and deflections. Finite element techniques can be employed to identify areas of both high stress, where there may be potential fatigue problems, and low stress where there may be potential for reducing weight. Material properties: A fundamental requirement for any durability assessment is knowledge of the relationship between stress and strain and fatigue life for a material under consideration. Fatigue is a highly localized phenomenon that depends very heavily on the stresses and strains experienced in critical regions of a component or structure.

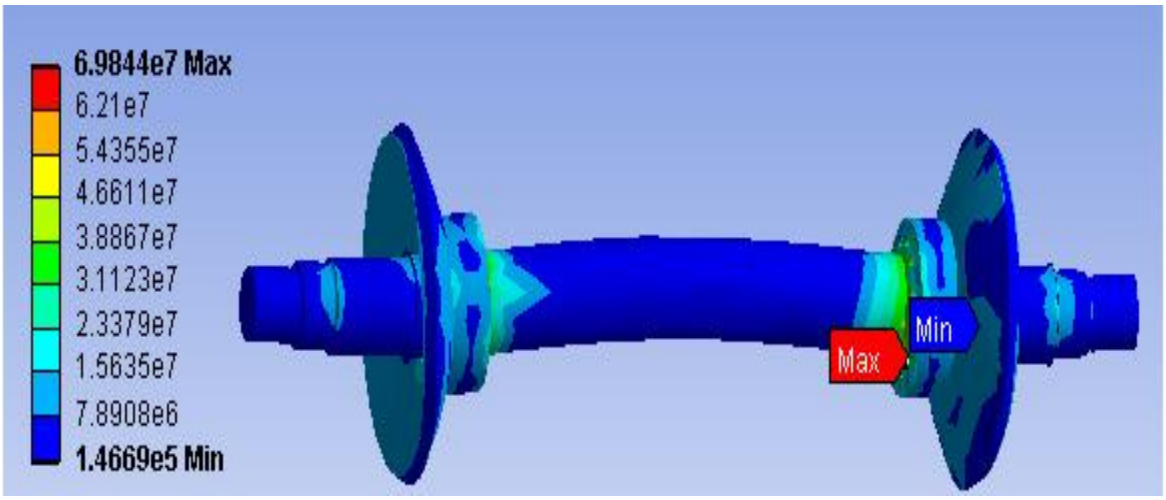

Figure 4-19 maximum shear stress

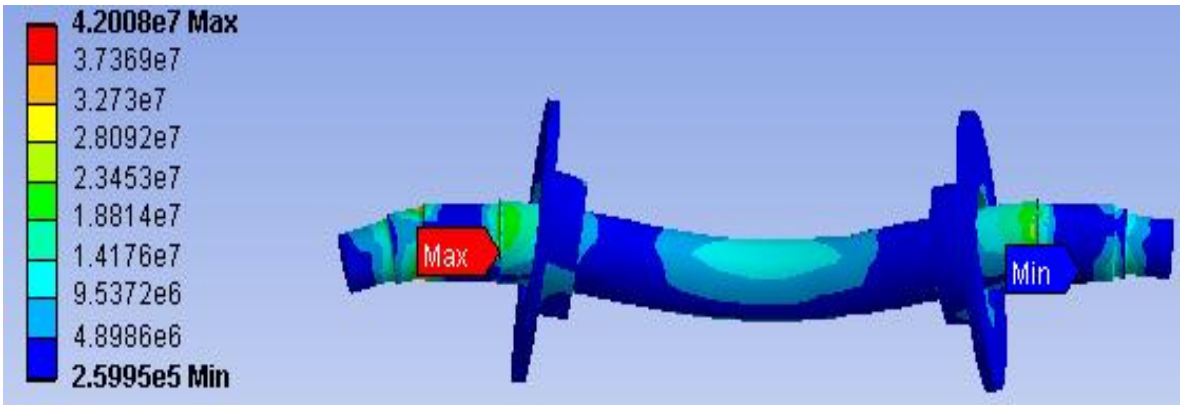

Figure 4-20stress intensity

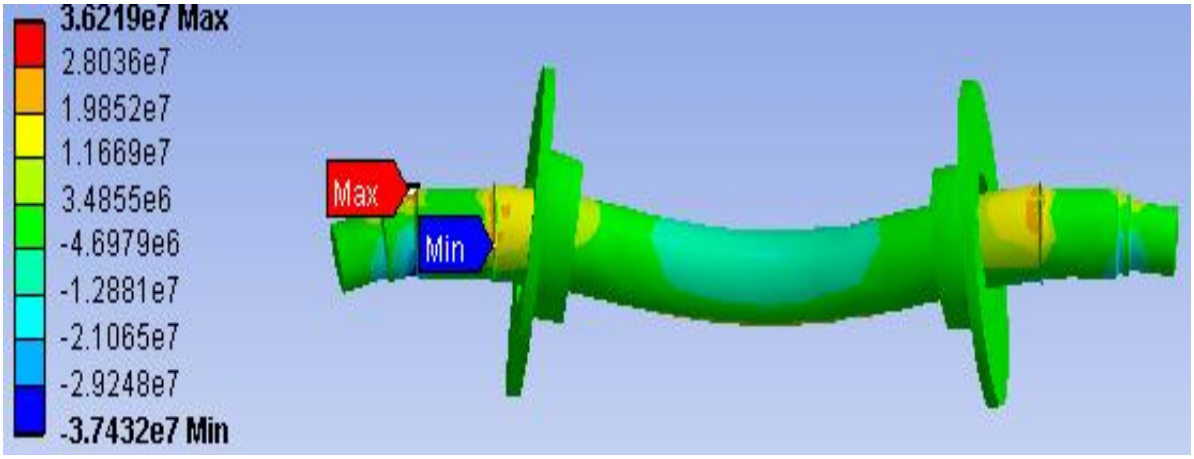

Figure 4-21Normal stress

Fatigue Life

Fatigue life can be defined as the number of stress cycles required to cause failure or Number of cycles that a material will sustain before failure occurs ; being a function of many variables; stress level, cyclic stress form and metallurgical condition of the materials are considered to determine fatigue life. From both software and manual the result is approximately the same.

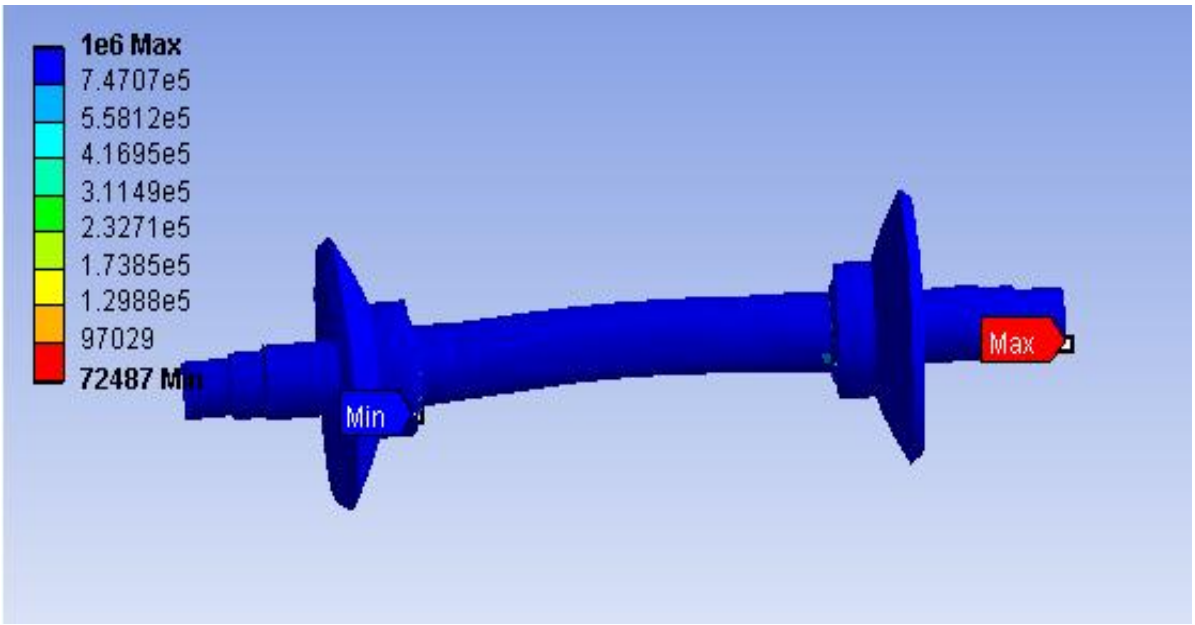

Figure 4-22life

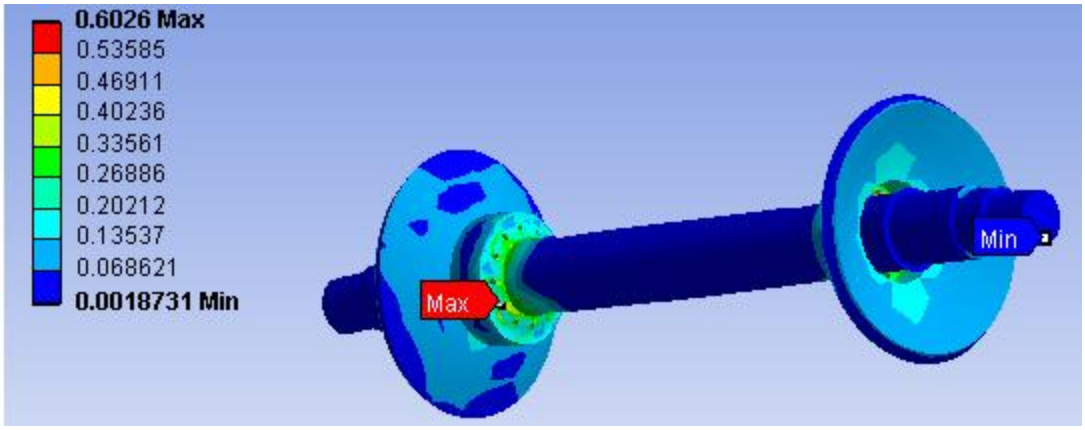

Figure 4-23 stress ratio

It is well known that the fatigue failure of axle depends on the fatigue load as well as the load ratio. These two fatigue loading parameters are related through the fatigue load ratio, R, which is the ratio of minimum to maximum fatigue load.

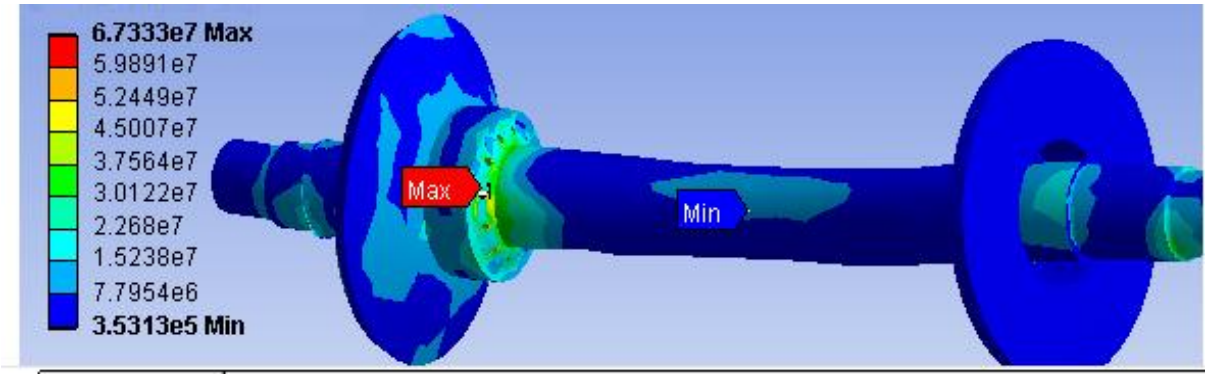

Figure 4-24 equivalent alternate stress

The equivalent alternating stress obtained from software is 67.33133Mpa.

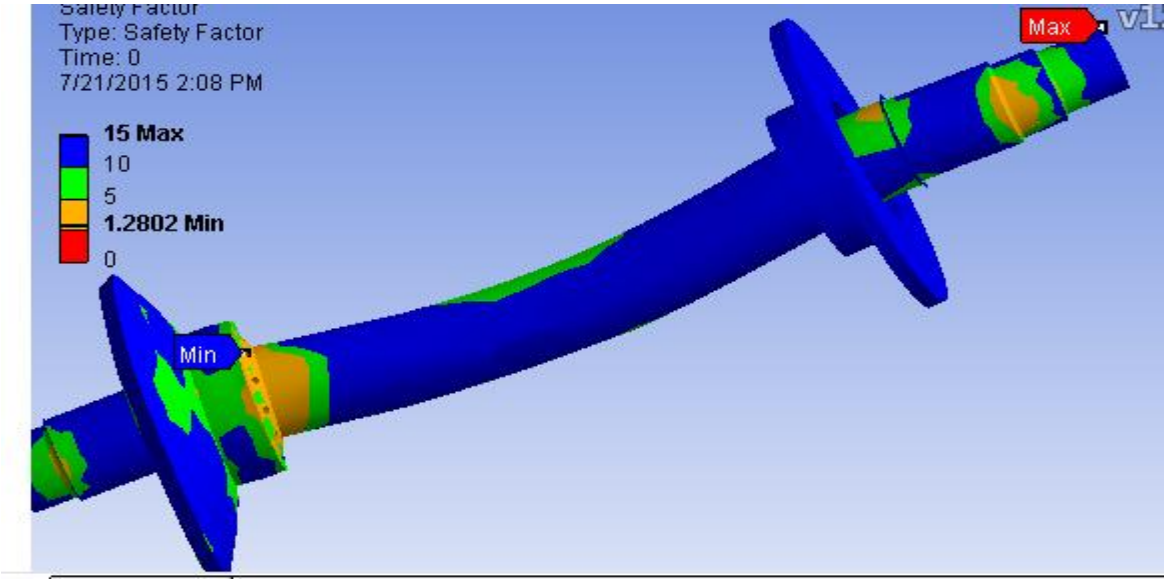

Figure 4-25 safety factor

Endurance Factor of Safety is calculated for High cycle Fatigue applications.

Endurance Factor of Safety = Endurance Strength / FE stress

Endurance Factor of Safety < 1 => Fail

Endurance Factor of Safety > 1 => Safe

Maximum Factor of Safety displayed is 15

Minimum Factor of Safety displayed is 1.2802 Fatigue Safety Factor, values less than one indicate failure before the design life has been reached. So the Factor of Safety 1.4>1 it is safe.

5.4 Results and discussion

This plot shows how the fatigue life results change as a function of the loading at the critical contact point for the axle components.

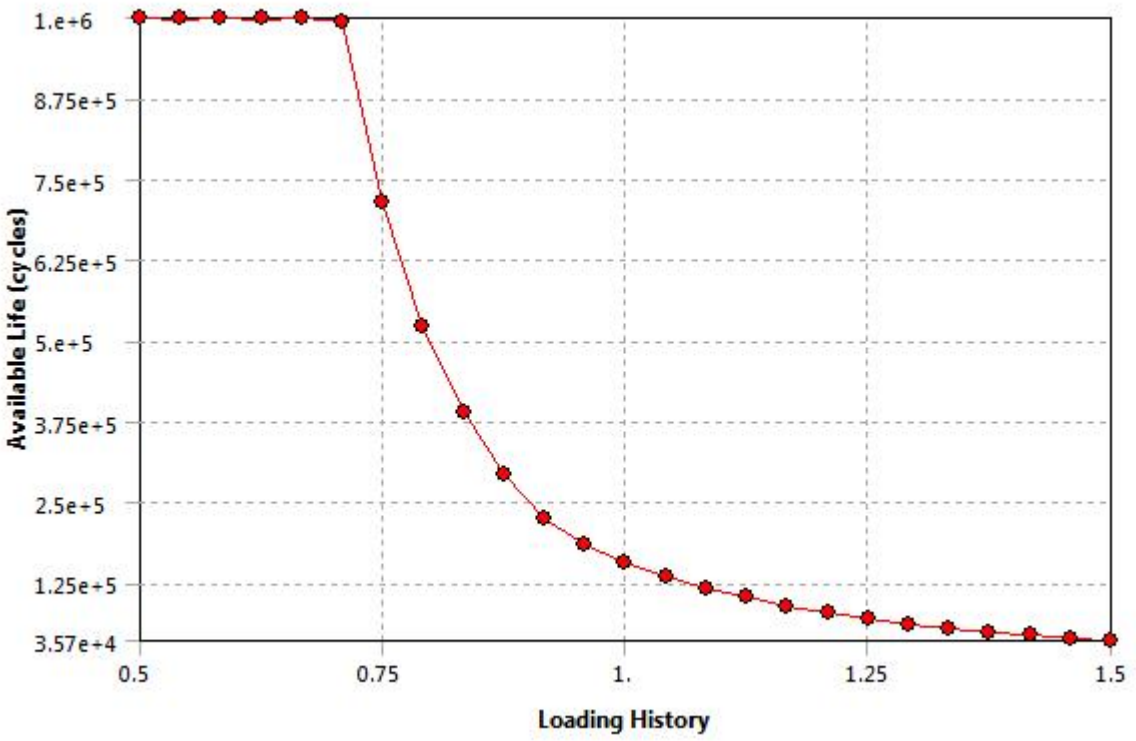

Figure 4-26 the sensitivity of fatigue life to applied loading

Fatigue Sensitivity shows how the fatigue results change as a function of the loading at the critical location on the model. The user may set the number of fill points as well as the load variation limits. For example, the user may wish to see the sensitivity of the model's life if the FE load was 50% of the current load up to if the load 150% of the current load. A value of 100% corresponds to the life at the current loading on the model. Around 70 %(6000000 of alternate stress) of loading the life is constant then after that it decrease exponentially because of cyclic loading. Shows how the fatigue results change with loading at the critical location on the model.

Sensitivity for life, damage, or factor of safety

Load variation limits

Number of fill points=25

Upper variation=150%

Lower variation=50%

From the sensitivity of available life with respect to loading, Specify a minimum base load variation of 50% (an alternating stress of 1450Nmm^{-2}) and a maximum base load variation of 200% (an alternating stress of 5800Nmm^{-2}).

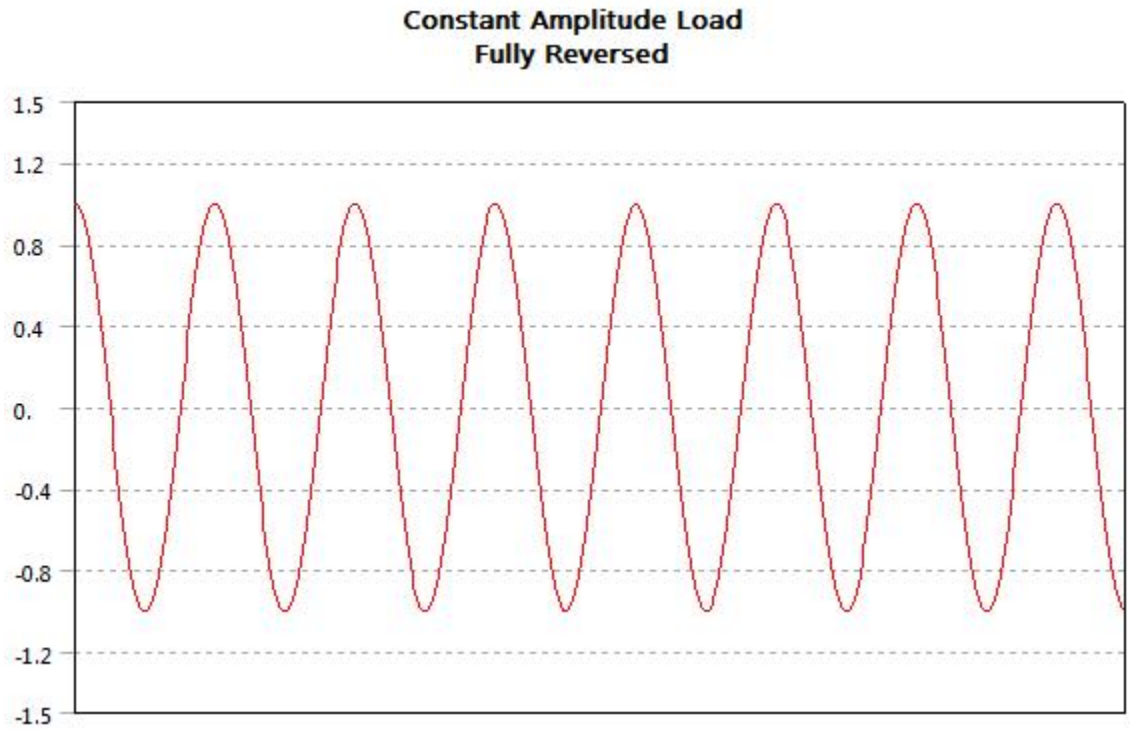

Figure 4-27 constant amplitude loading

Loading is of constant amplitude because only one set of FE stress results along with a loading ratio is required to calculate the alternating and mean values. Constant amplitude, proportional loading is the classic, “back of the envelope” calculation describing whether the load has a constant maximum value or continually varies with time. Common types of constant amplitude loading are: Fully reversed (apply a load, then apply an equal and opposite load; a load ratio of –1).

Table 4-7 Alternate Stress vs. number of cycles

Alternating Stress Pa	Cycles	Mean Stress Pa
3.999e+009	10	0
2.827e+009	20	0
1.896e+009	50	0
1.413e+009	100	0
1.069e+009	200	0
4.41e+008	2000	0
2.62e+008	10000	0
2.14e+008	20000	0
1.38e+008	1.e+005	0
1.14e+008	2.e+005	0
8.62e+007	1.e+006	0

The table shows the most fatigue affect is caused by alternative stress. It was found that increasing the mean load has a deleterious effect on the fatigue life for a fixed fatigue load range. Fatigue life decreases as mean load increases for a fixed fatigue load range. Structural members subjected to in-service cyclic loads exhibit a fatigue behaviour that generally depends on the mean stress values. For a given fatigue load range a tensile mean normal stress has a detrimental effect on fatigue strength, whereas, in general, a compressive mean normal stress has a beneficial effect. Various criteria have been proposed to deal with the mean stress effect on fatigue life, such as Soderberg, Goodman and Gerber diagrams. Mean stress has no significant effect as shown in the table.

Stress Life Interpolation: Within a Stress Life analysis, there are three different methods by which interpolations can be done; log-log, semi-log and linear. Results will vary due to the interpolation method used. If our component is in low cycle region then we have to consider strain-life approach. If our component is in high cycle region then we consider stress-life approach. The axle is in high cycle region so we considered stress-life approach which in turn tells that our component is in infinite life region.

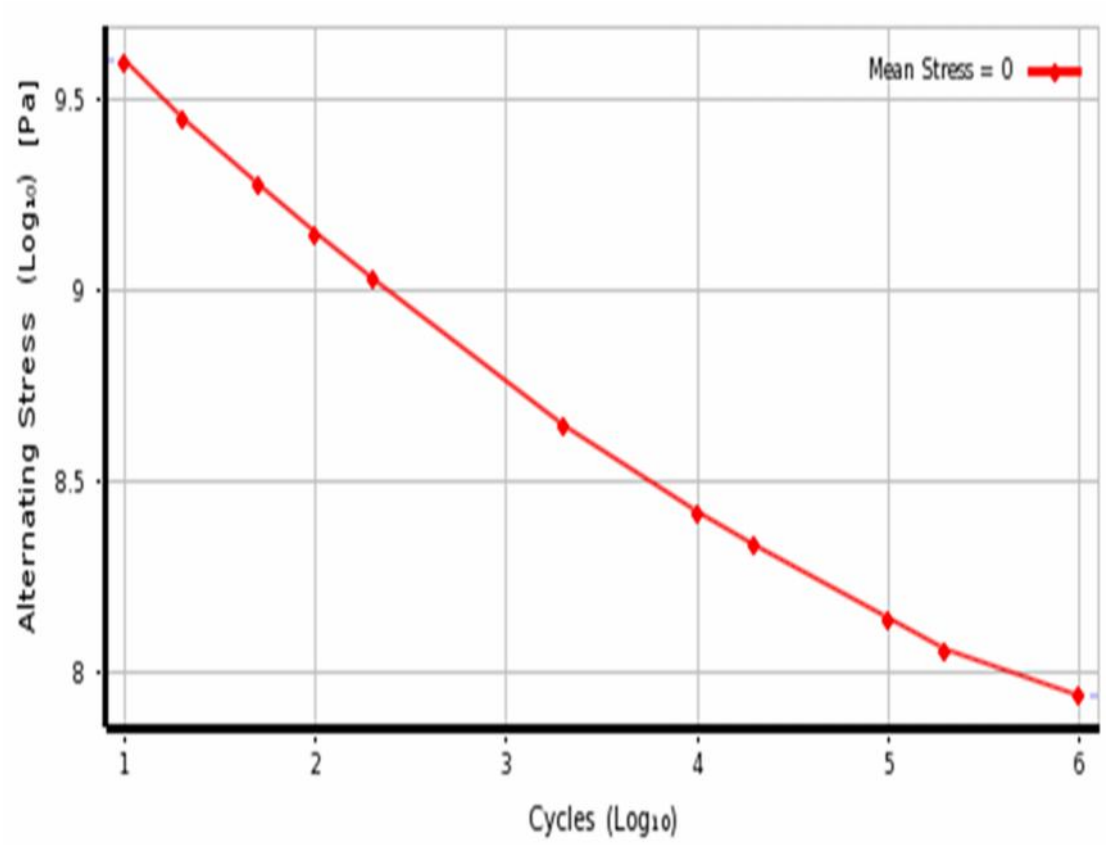

Figure 4-28alternating stress versus number of cycles [log-log relationship]

From above figure the results section plots the fatigue life, N, as a function of the stress amplitude applied, S. From the graph, we can see that there is a marked decrease in fatigue with increasing stress amplitude, which is in accordance with our theoretical assumptions. A continuously decreasing S-N response, S decreases continuously with N. When plotted on a log-log scale, an S-N curve can be approximated by a straight line.

For ferrous metals this range is from $1x10^3$ to $1x10^6$ cycles. S-N method does not work well in low-cycle application, where the applied strain have a significant plastic component. Fatigue strength: stress at which fracture occurs after specified number of cycles (e.g. 10^6). These curves however have certain limitations. They only provide fatigue life without giving any indication about cycles needed for crack initiation and propagation.

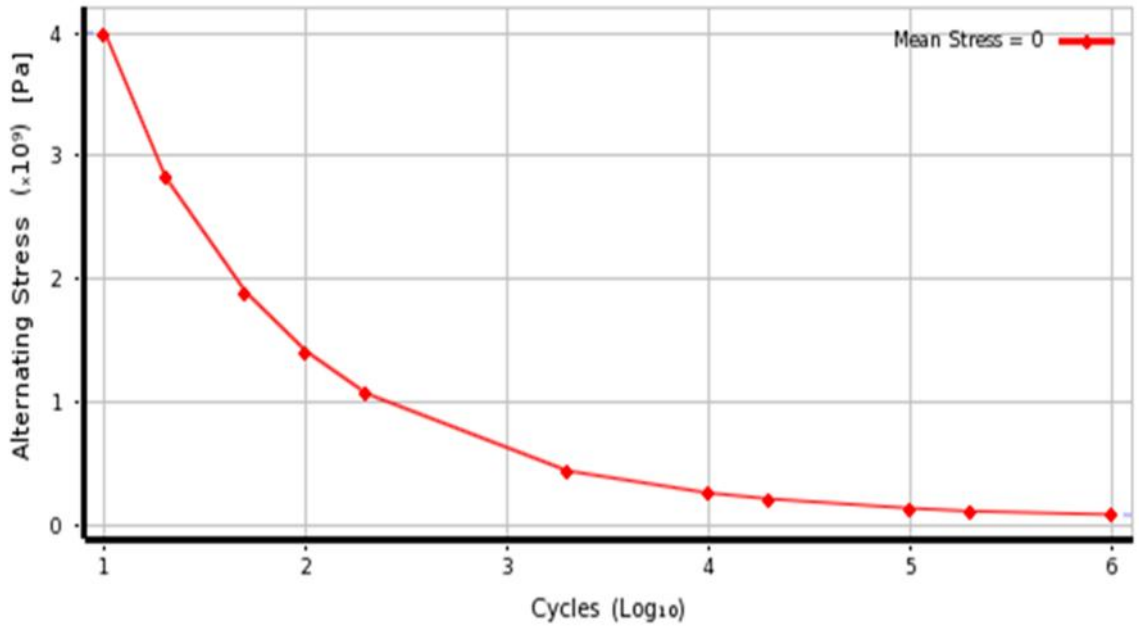

Figure 4-29 alternating stress versus number of cycles [semi log-log relationship]

During semi log-log it is exponentially decreasing curve.

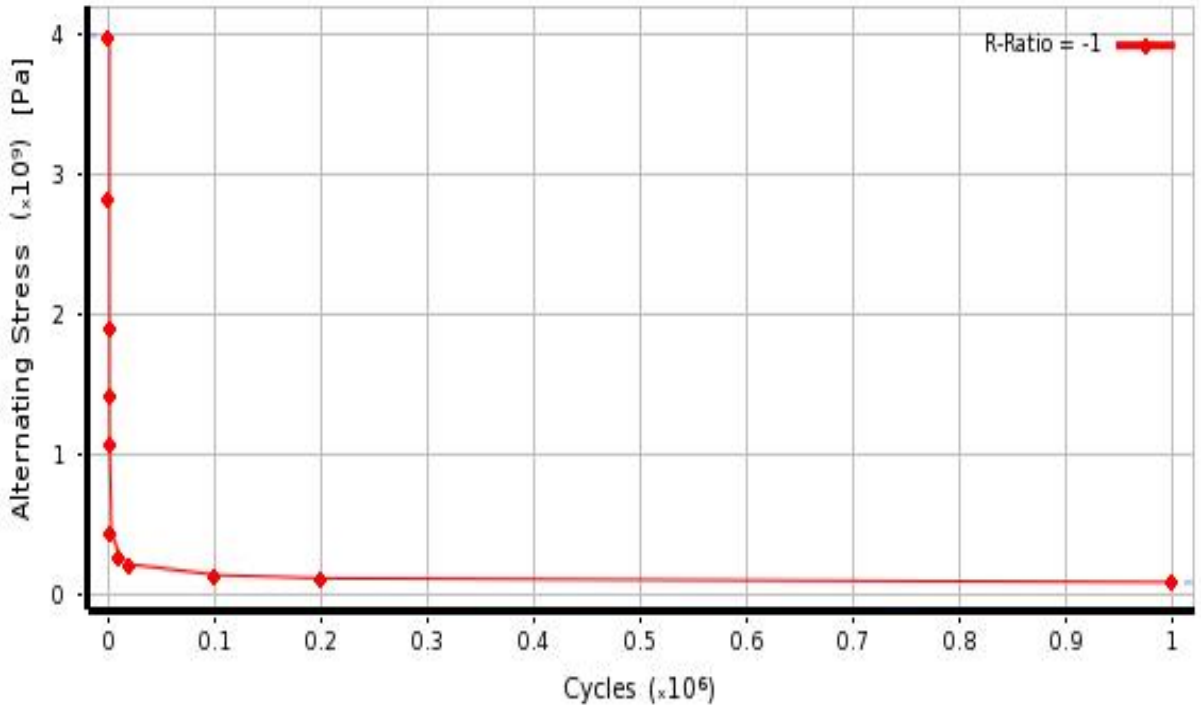

Figure 4-30 alternating stress versus number of cycles [linear relationship]

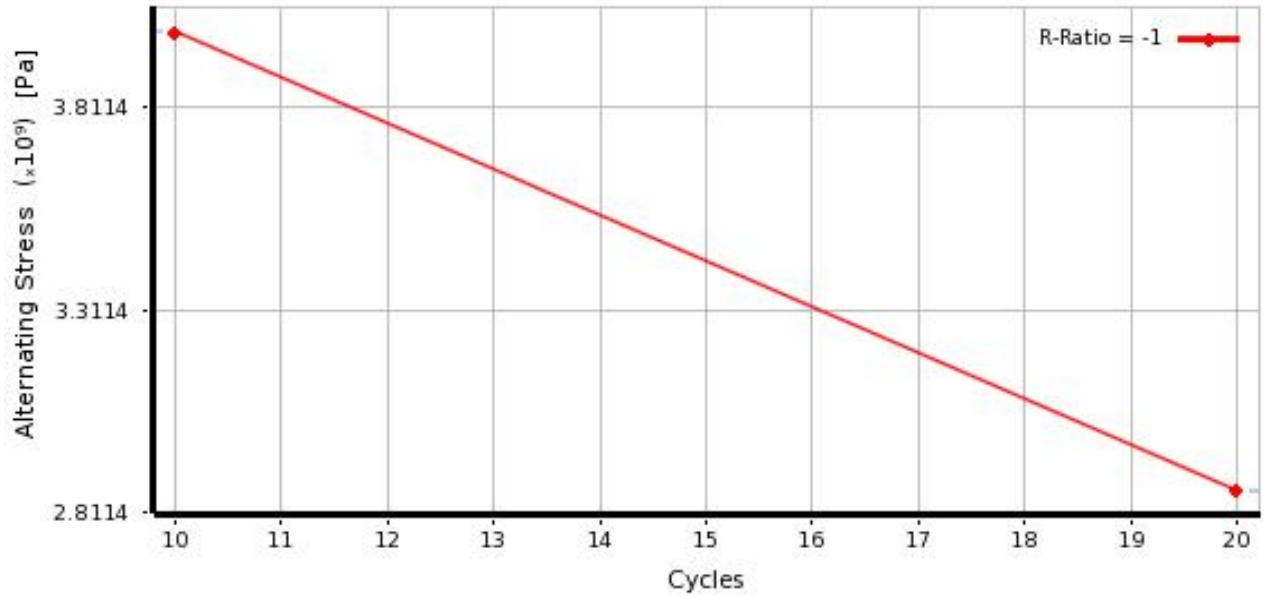

Figure 4-31 alternating stress in tabular form

R=-1 because of alternative stress and fully reversed

Continuously decreasing curve with constant stress ratio. S-N curves for different load ratio values (varying the load ratio will result in varying the ratio of the mean to alternating stress components).

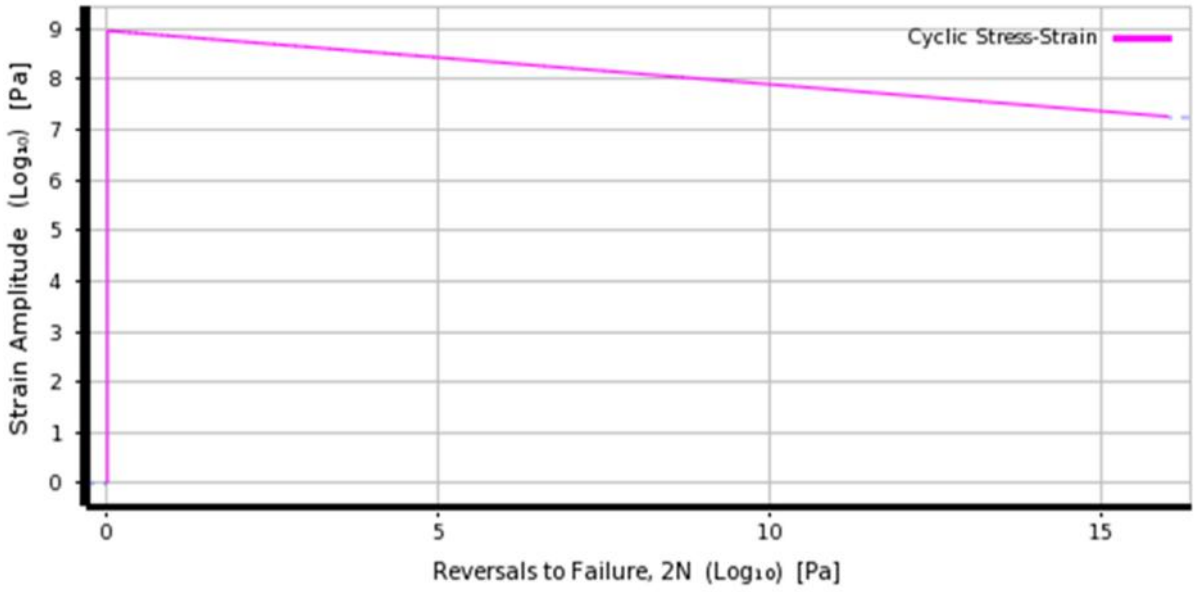

Figure 4-32strain amplitude versus to number of cycles

If N=constant (N=0), then strain amplitude increase up to the maximum.

When N≠0 (Constant), As N increase continuously then strain amplitude decreases continuously.

Mean Stress Corrections for Strain Life

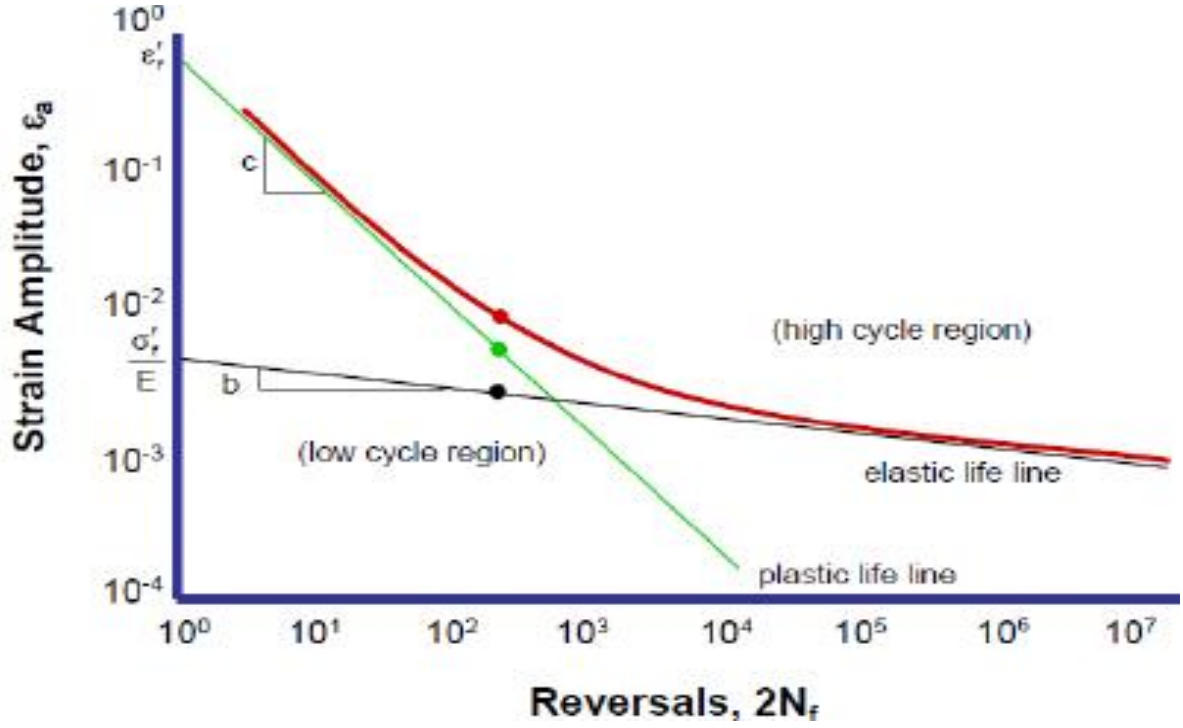

Figure 4-33 strain versus reversal to failure

b=fatigue strength exponent is the slope of elastic-strain life line. Fatigue strength exponent b is the slope of the elastic-strain line, and is the power to which the life 2N must be raised to be proportional to the true-stress amplitude.

c=fatigue ductility exponent is the slope of plastic life line. The fatigue ductility coefficient is the true strain required to cause failure in one reversal i.e. the intercept of the plot:

The slope of the plastic strain-life line may also be considered a fatigue property and is called the fatigue ductility exponent 'c'. It can be defined as the power to which the life (in reversals) must be raised to be proportional to the plastic strain amplitude. Fatigue ductility exponent c is the slope of the plastic-strain line in Fig. 5–22 and is the power to which the life 2N must be raised to be proportional to the true plastic strain amplitude. If the number of stress reversals is 2N, then N is the number of cycles.

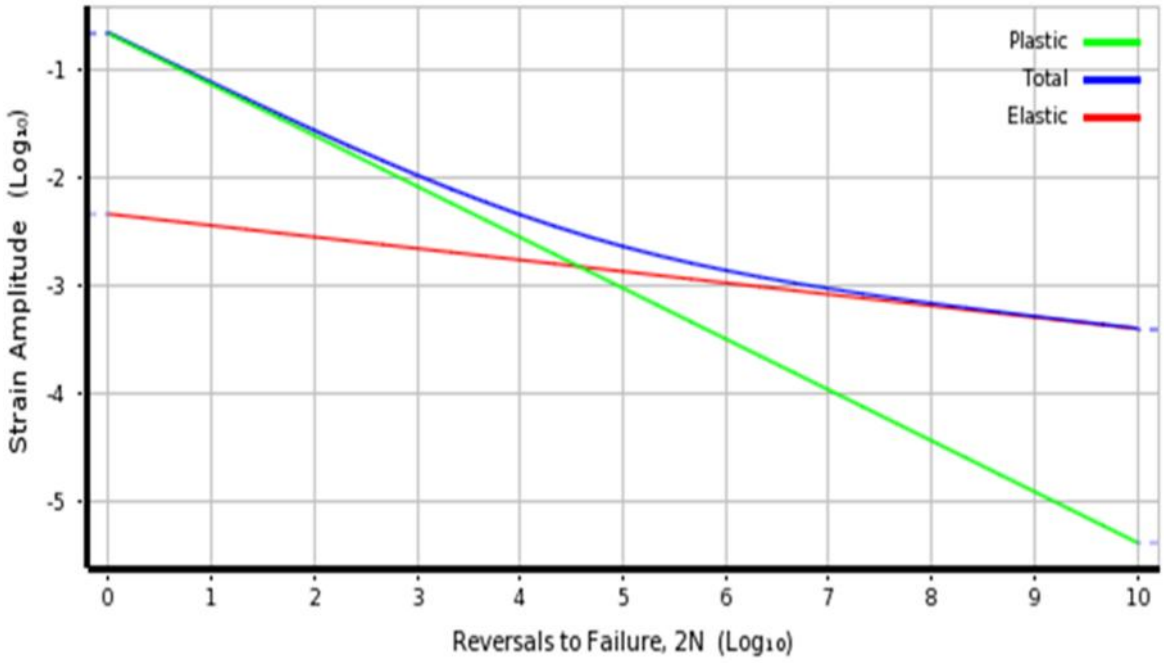

Figure 4-34 strain amplitude versus to number of cycles

The life where elastic and plastic components of strain are equal is called the transition fatigue life: 2Nt is the intersection point of plastic and elastic on the graph. For lives less than 2Nt the Deformation is mainly plastic, whereas for lives larger than 2Nt the deformation is mainly elastic. Since total life is close to elastic then it is elastic life .At large strains or short lives, the plastic strain component is predominant, and at small strains or longer lives the elastic strain component is predominant. Plastic deformation taking place during cyclic loading causes microstructural changes such as structure and density of dislocations. When the stress at the discontinuity exceeds the elastic limit, plastic strain occurs. If a fatigue fracture is to occur, there must exist cyclic plastic strains. Now, from Fig. 5–23, we see that the total strain is the sum of the elastic and plastic components. Therefore the total strain amplitude is half the total strain range.

Table 4-8 Software & mathematical comparison

ANSYS Result	Numerical Result	ERROR
Equivalent(von-mises)stress=46.787Mpa	73.644Mpa	20%
Safety factor=1.2802	1.4	9.75%
Normal stress=41.385Mpa	44.9Mpa	7.83%
Equivalent alternate stress=46.6685Mpa	69.654Mpa	21.3%
Infinite life	Infinite life	

From this table software result and analytic results are almost approach to each other.

Equivalent stress vary along the geometry of the axle and due to this the result is vary.

From above Table.5.2 it is clear that, the fatigue analysis of axle gives close results by Analytical and FEA approach. The FEA analysis is very useful tool. Also, to change the material having low value of $\pm_{yt}$ then to reduce the value of fatigue factor of safety for saving cost of material. Software used for fatigue analysis CATIA V5, ANSYS12 which gives moderate results.

Chapter 6

CONCLUSION, RECOMMENDATION AND FUTURE WORK

6.1 Conclusion

The static analysis of railway axle is carried out to find out the deformation in loading conditions and it is found to be maximum 0.0000462104mm. The value of stress found to be more at the critical section of the axle as indicated by red colour. Hence possibility of failure is more at that section compared to other section of axle. Initially a free body diagram is represented for the power axle based on loads coming on the structure during operation and theoretical calculations are calculated for the loads using De-Goodman criteria. By considering different sections for theoretical moment, torque and stress calculations using numerical analysis carried out & we checked the safety factor of the axle. The cyclic load leading to fatigue failure was caused by the mass in motion, brake force and gear force. The mechanical design and material selection of the axle is appropriate for its intended service. The paper presents the summary of stress and fatigue analysis in railway front axle. In this paper the main approach is to get better result on the account of life cycle of axle and also study the behaviour of stress and fatigue on axle. Forces that contribute to fatigue failure of railway axle are analyzed and investigated in detail. All forces that act on axle are determined. Fatigue factor of safety calculated manual is 1.4 and by FEA 1.2802 these values are almost the same. The number of life cycles are calculated by De-Goodman method are $1.65X10^6$ cycles and by using FEA it will show safely run at $1*10^6$ cycles. So, it will show infinite life cycle checked at high cycle fatigue. Also, it is clear from above results, Von-Mises stress value by analytical approach 73.26 N/mm2 which are nearly same by using FEA approach having difference of 20% in both results which is acceptable range.

The effect of alternate stress is investigated. From the result of equation (4.11) & (4.12), logarithmic alternating / mean stress values 7.872 Pa & 8.004 Pa which are less than material alternating stress value of 9.5 Pa. So, conclude that, the working alternating / mean stress within limit value and increased fatigue strength for infinite life below material endurance strength limit. The materials used in analysis is selected and chemical composition and mechanical property is explained. Finite Element verification using ANSYS software is carried out to check the stress and deformation conditions and further analyses carried out with rotational load corresponding to 70KMPh. FEM analysis is very efficient and simple

method for achieving stresses at different loading condition according to forces applied to the axle from the static analysis. The use of numerical method such as Finite Element Method now a day commonly used to gives detail information about structure or component.

6.2 Recommendations

The primary function of the axle is to provide to transmit driving torque to the wheels, as well as to maintain the position of the wheel relative to each other and to the vehicle body. The axle in this system must also bear the weight of the vehicle plus any cargo. According to [6 & 8] brake disc and curves are another source of axle loading. Brake disc loads as action and reaction force whereas curves acts as lateral force on the axle. More over in order to resist bending or braking, the axle is made from AISI1050 structural steel. From this point of view AISI1050 (carbon steel) is more welded than chromoly steel with tools normally found outside a professional welding shop. Furthermore, a 4130(chromoly steel) has an enough potential to be used as an axle materials from its excellent strength to weight ratio, stronger and harder than AISI1050 (carbon steel) but not easily welded (need pre and post weld thermal treatment to avoid cold cracking).materials used for the axle is different carbon composition of steel. From this regard, it is possible to conclude that the result output of AISI1050 of this material can give best result for axle material for simplicity to welding problem than chrome steel. We can minimize the possibility of fatigue failure by proper design of structural components (axle). The recommendation is to standardization of the axle and to limit stress concentration that could be very dangerous during life of component; a special care should be taken to guarantee overlap of components on seat of the axle, since this matter directly affects the stress concentration.

6.3 Future Work

In this thesis work fatigue Analysis is studied using analytical and FEM numerical method, it can be further studied by performing experiments for a better result in addition to that other influencing factor is not studied in this paper. So this work is restricted to the specified cases. However, this paper can be extended to other situation listed below. Further numerical method investigations should be conducted on:

The effect of dynamic force on axles

Effect of environmental condition on the on axles.

Effect of misalignment and sliding speed on surface contact stress of axle bearings

REFERENCE

[1] Paul W.Winter and Don A.Macinnes, 1993. Fatigue under Variable

Amplitude Loading: A New Approach, Volume II, Safety and Reliability, AEA Technology, pp. 99-106.

[2] Wulpi DJ. Failures of shafts. In: Failure analysis and prevention. ASM metals handbook, vol. 11. Metals Park (OH): American Society for Metals; 1986. p. 459–82.

[3]. Way, S., Pitting Due to Rolling Contact, J. Appl. Mech., vol. 2, pp. A49 A58, 1935.

[4]. A.Goksenli, I.B. Eryurek _Failure analysis of drive shaft. 'Engineering failure analysis 16 (2009) 1011-1019

[5] K. Hirakawa, K. Toyama and M. Kubota, The analysis and Prevention of failure in railway axles, Int. Journal Fatigue, 20 (1998) 135-144.

[6]. S. Beretta*, M. Carboni, G. Fiore, A.Lo Conte, corrosion-fatigue of A1N railway axle steel exposed to rainwater. (2010)952-961(Elsevier)

[7]. [Shigle 8th edition, page 271-300]

[8].Alfredsson, B. A study on contact fatigue mechanisms, Doctoral thesis, Department of Solid Mechanics, Royal Institute of Technology, Stockholm, Sweden, 2008.

[9]. Murakami, Y., Takada, M. and Toriyama, T., Super-long life tension-compression fatigue properties of quenched and tempered 0.46% carbon steel. Int. J. Fatigue, Vol. 20 (1998), pp. 661–667.

[10]. Murakami, Y., Endo, M., Journal of Basic Engineering, v16, 163-182, 1994.

[11]. S. Berettaa,*, A.Ghidinib, F.Lombardoa, b, Fracture mechanics and scale effects in the fatigue of railway axles. (2005)195-208(Elsevier)

[12].S. Berettaa, M. Carbonia, A. Lo Contea*, D.Regazzia, S. Trasattib, M. Rizzib, Crack growth studies in railway axles under corrosion fatigue: full-scale experiments and model validation. (2011)3650-3655(elsevier)

[13].M. Madia, S. Beretta, and U. Zerbst, An investigation on the influence of rotary bending and press fitting on stress intensity factors and fatigue crack growth in railway axles. Engineering Fracture Mechanics 2008. 75: p. 1906-1920.

[14]. Hillmansen, S, & Smith, R an Intelligent measurement of the in service rail vehicle axle environment, In Proceedings, Implementation of Heavy Haul technology for Network Efficiency, May 5-9, 2003, Dallas, USA, pp. f.11-f.17, 2004

[15].S. Beretta*, M. Carboni, Variable amplitude fatigue crack growth in a mild steel for railway axles: Experiments and predictive models. (2011)848-862(elsevier)

[16]. Bing Yang*, Yong Xiang Zhao, Experimental research on dominant effective short fatigue crack behavior for railway LZ50 axle steel (2012)71-78(elsevier)

[17].S. Beretta, et.al Application of fatigue crack growth algorithms to railway axles and comparison of two steel grades. Proceedings of the Institution of Mechanical Engineers, 2004. 218: p. 317-326.

[18].TaizoMakinoa,*, Takanori katoa, Kenji Hirakawa, Review of the fatigue damage tolerance of high-speed railway axles in japan. (2011)810-825 (elsevier)

[19]. Zerbst, U., Vormwald, M., Andersch, C.: The development of a damage tolerance concept for railway components and its demonstration for a railway axle. Eng. Fract. Mech. 72, 209–239 (2005) Engineering 11 (1871) March 17, pp. 199-200 and subsequent issues.

[20]. M. Novosad, et al, Fatigue Test of Railway Axles". Procedia Engineering 2, 2010:p. 2259-2268

[21]. Voskamp, A.P., ASTM Special Technical Papers, v 1327, 152-166, 1998.

[22]. 18. Lorösch, H-K., "Influence of Load on the Magnitude of the Life Exponent for Rolling

Bearings", In: Rolling Contact Fatigue Testing of Bearing Steels, ASTM STP 771 (Edited by J. J. C. Hoo), Phoenix, May 12-14, 1981, American Society for Testing and Materials, Philadelphia, 1982.

[23]. Fuji, Y., Maeda, K., Wear, v252, 799-810, 2002.

[24]. Dawson, H. P., Journal Mechanical Engineering Science, v 9(1), 67-80, 1967.

[25]. I. Le May, A. K. Koul, and R. V. Dainty t, Fracture Mechanisms in a Series of

Locomotive Axle Failures. Materials Characterization, 1991. 26: p. 235-251.

[26]. Viktor Gerdun a, et al., Failures of bearings and axles in railway freight wagons. Engineering Failure Analysis, 2007. 14: p. 884–894.

[27]. H. F. Moore, A study of fatigue cracks in car axles. Bulletin No. 165 Engineering Experiment Station, 1927.

[28]. M. Bayraktar, N. Tahrali, and R. Guclu, Reliability and fatigue evaluation of railway axles. Journal of mechanical science and technology 2009. 24(3): p. 671- 679.

[29]. U.zerbst, et al., Safe life and damage tolerance aspects of railway axles- A review. Engineering Fracture Mechanics, 2013. 98: p. 214-271.

[30]. S. Beretta, A. Ghidini, and F. Lombardo, Fracture mechanics and scale effects in the fatigue of railway axles. Engineering Fracture Mechanics, 2003. 72: p. 195– 208.

[31]. R. A. Smith, Railways and materials: synergetic progress. Iron making and steel making, 2007. 35: p. 505-513.

[32]. Sulochana and U.K. Joshi, Study on fatigue failure and stress analysis with safe life on railway axle- A review. International journal of Emerging Trends in Engineering and Development, 2013. 2(3): p. 210-215.

[33]. M. Luke, et al., Fatigue crack growth in railway axles: Assessment concept. Engineering Fracture Mechanics, 2011. 78: p. 714-730.

[34]. A.S. Watson and K. Timmis, A method of estimating railway axle stress spectra. Engineering Fracture Mechanics, 2011. 78: p. 836–847.

[35]. Japanese Industrial Standards JIS E 4501-1995 Railway Rolling Stock – Design Methods for Strength of Axles

[36]. Japan Association of Rolling Stock Industries Standards JRIS J 0401-2007 Rolling Stock – Induction-Hardened Axles for High Speed Vehicle

[37]. Cummings, H.N., Stulen, F.B. and Schulte, W.C., Tentative fatigue strength reduction factors for silicate-type inclusions in high-strength steels. Proc. ASTM, Vol. 58 (1958) pp. 505-514.

[38]. Forrest, P.G., Fatigue of Metals. Pergamon Press, Oxford (1962). 10. Ransom, J.T., The effect of inclusions on the fatigue strength of SAE 4340 steels. Trans. Am. Soc. Metals, Vol. 46 (1954), pp. 1254–1269.

[39]. De Freitas M., and François D., Analysis of fatigue crack growth in rotary bend specimens and railway axles, Fatigue. Fract. Engng. Mater. Struct, 18 (2) pp. 171-178 (1995).

APPENDIX

Mean Stress Correction (Strain Life)

$$\frac{\Delta £}{2} = \frac{\pm f - \pm_{mean}}{E}(2Nf)^b + £f'(2Nf)^c$$

$where, \frac{\Delta £}{2} = Total\ strain$

$E = \text{mod}\ ulusofelas\ ticity$

$\Delta \pm = 2 * thestressa\ mplitude$

$Nf = numberofcy\ cletofailu\ re$

$£f' = fatigueduc\ tilitycoef\ ficient$

$c = fatigueduc\ tility\ \text{exp}\ onent$

$2Nf = numberofre\ versaltofa\ ilure$

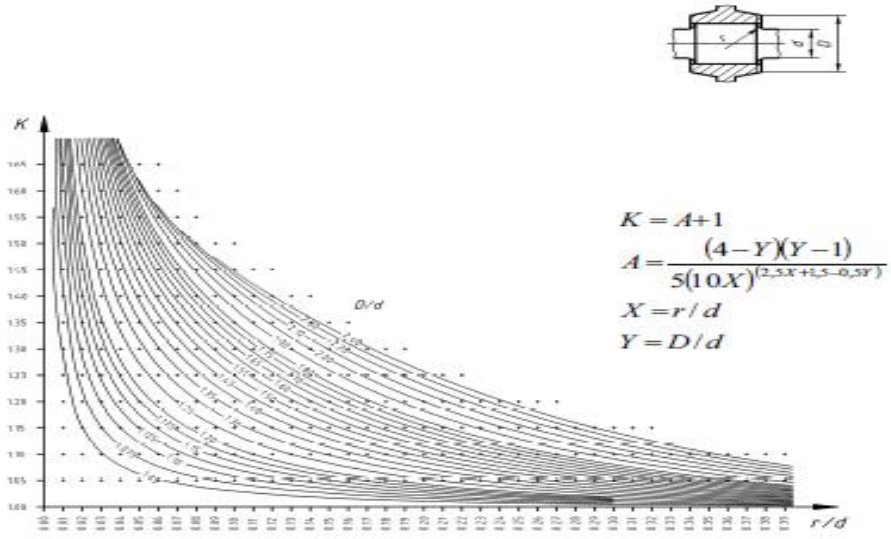

Fig Fatigue stress concentration factor K as a function of D/d and r/d (at the bottom of the transition between two cylindrical parts)

$$\frac{D}{d} = \frac{177}{144} = 1.2$$

$$Y = 1.25\ \&\ X = 0.14$$

$$B = \frac{-1.2 * 0.14^2 + 37 * 0.14}{1.25^6} + 1.74 = 2.92$$

$$A = \frac{(4 - 1.25)(1.25 - 1)}{5(10 * 0.14)^{(2.5*0.14+1.5-0.5*0.14)}} = 0.06428$$

$$k = A * B + 1 = 0.06428 * 2.92 + 1 = 1.2$$

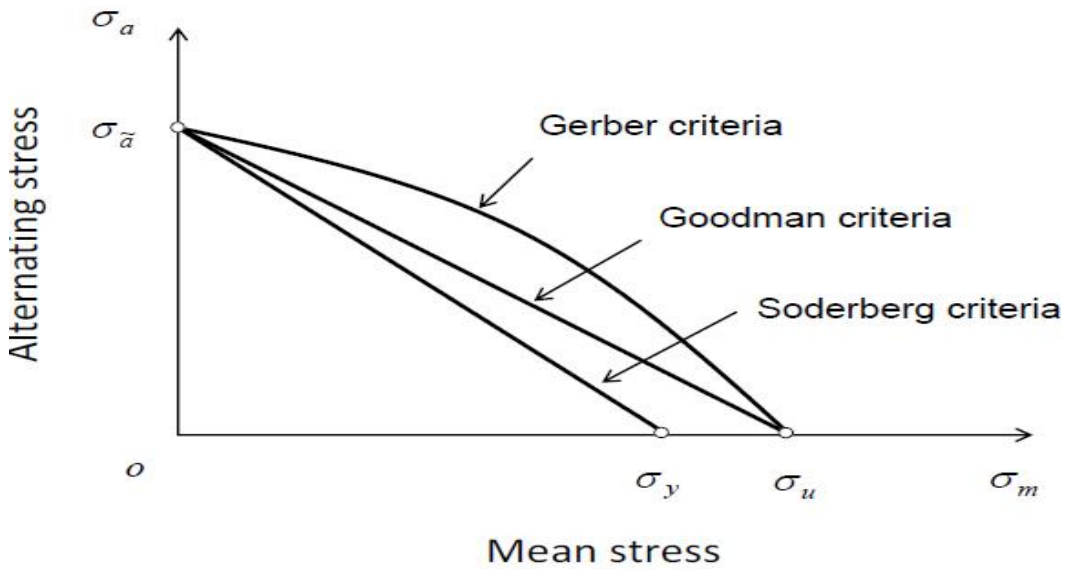

Fig The mean stress effect on fatigue life: Soderberg, Goodman and Gerber criteria

Range of railway axle

overall length, L/mm	distance between two journal centers, L1/mm	axle journal length, L2/mm	dust collar length, L3/mm	length of wheel seat,L4/mm	axle journal diameter, D1/mm	wheel seat diameter, D2/mm	axle body diameter, D3/mm	alxe load/t
2062-2356	1905-2007	187-305	44-79	192-198	100-180	155-241	138-215	12-35

Source on Alibaba.com

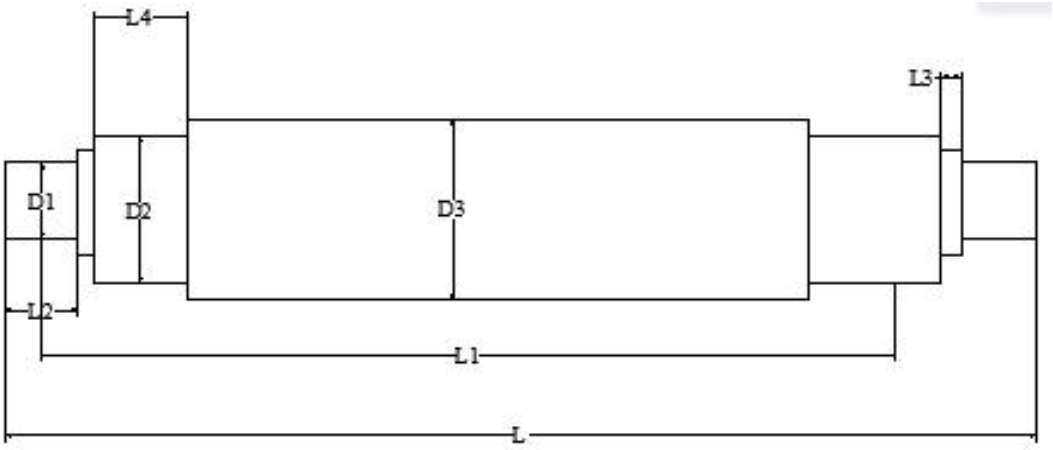

ANNEX

Technical Description of RW25G Soft Berth Passenger Car

3.3.1 General Technical Specification

Car strength complies with TB/T1335-1996《Railway vehicles Strength design and test evaluation specification》.

Vehicle dynamic performance complies with GB/T 5599-1985 《Railway Vehicle Dynamics Performance Evaluation and test identification norms》.

Vehicle gauge complies with GB146.1-198《Standard railway rolling stock gauge>>

Service life: 30 years

Maintenance period:

_ Maintenance back to factory: 2.4 (±0.6) M Kilometers or 10years.

_ Maintenance in deport: 0.6(±20) M kilometers or 2.5years.

Conditions of Use:

_ Maximum configuration: 20car per train set

_ Ambient temperature: -40℃ ~ +40℃

_ Maximum relative humidity ≤95%

_ Platform height, Suitable for platform height with 300mm、500mm and1250mm, distance between platform edge and railway center is 1750mm.

_ Maximum line gradient ≤30‰

3.3.2 Main technical specification

Railway gauge 1435mm

Maximum operation speed 120km/h

Emergency brake distance on straight line (with 30% overload and with initial Speed 120km/h) ≤800m

Minimum negotiable curve

Single car 100m

Coupling 145m

Ride index W≤2.5

Axle load ≤17t

3.3.3 Main dimension

Carbody length 25500mm

Carbody width Approx 3105mm

Height between rail top to car top (empty car) 4433mm

Vehicle center distance 18000mm

Height from rail top to coupler center (empty car) 880

+10

-5 mm

Height from rail top to inter car crossing pedal (empty car) 1333mm

Height from rail top to floor surface (empty car) 1283mm

Carbody center plate to rail top (empty car) 780mm

ADDIS ABABA UNVERSITY

Addis Ababa Institute of Technology

School of Mechanical and Industrial Engineering

I, the undersigned, declare that this thesis is my original work and has not been presented for any degree in any university and all the sources of materials used for the thesis have been duly acknowledged.

Name	.....	.....
Shoma Tadesse	Signature	Date